VIRGINIA GEOLOGICAL FIELD CONFERENCE 2025

HOLOCENE BARRIER DYNAMICS AND MANAGEMENT ON THE EASTERN SHORE OF VIRGINIA

20–22 MARCH 2026

FIELD TRIP GUIDE

Trip Leader: Christopher Hein (Virginia Institute of Marine Science [VIMS])

Contributing Authors (alphabetical): Allyson Boggess (VIMS), Kayla Cahoon (North Carolina Geological Survey), Daniel Ciarletta (U.S. Geological Survey), Elizabeth Davis (VIMS), Michael Fenster (Randolph-Macon College), Ioannis Georgiou (The Water Institute), Michelle Harris (Moreno Valley College), Emily Hein (VIMS), Katherine Kivimaki (VIMS), William McCormick (VIMS), Justin Shawler (U.S. Army Engineer Research and Development Center)

VGFC Leadership Team: Callan Bentley (President), Tyler Sauer (Vice President), Linda Morse (Treasurer), David Hawkins (Secretary)

VGFC Virginia Geological Field Conference

Chincoteague Bay Field Station

VIMS | William & Mary
Virginia Institute of Marine Science

FIELD TRIP ITINERARY

DAY #1: FRIDAY, 20 MARCH 2026

GATHERING AND BUSINESS MEETING

17:00 – 18:30: VGFC Business Meeting
(Chincoteague Bay Field Station Auditorium)

18:30 – 20:00: Dinner (Chincoteague Bay Field Station Cafeteria)

20:00 – 20:30: Regional and Field Trip Overview Presentation (C. Hein)

DAY #2: SATURDAY, 21 MARCH 2026

WALLOPS-ASSAWOMAN, CHINCOTEAGUE, AND ASSATEAGUE ISLANDS

06:30 – 08:00: Breakfast (Chincoteague Bay Field Station Cafeteria)

08:00 – 08:30: Transit to Wallops Island

08:30 – 09:15: Stop #1: Wallops Island Overview (central radar stand overlook)

09:15 – 09:45: Stop #2: Developed and undeveloped barrier islands: Southern Wallops and Assawoman

09:45 – 10:30: Stop #3: Beach nourishment borrow site (north-central Wallops Island)

10:30 – 10:45: Restroom stop at X86 building

10:45 – 11:15: Transit to Chincoteague Island

11:15 – 11:45: Stop #4: Chincoteague Inlet: Mariner's Point, Curtis Merritt Harbor

11:45 – 12:15: Stop #5: Origin of Chincoteague Island: Donald J. Leonard Park

12:15 – 13:00: Stop #6: Progradation of Chincoteague Island: Hallie Whealton Smith Dr or Teal Lane or Taylor Street

13:00 – 14:00: Stop #7: Lunch at The Chincoteague Center (6155 Community Drive, Chincoteague)

14:00 – 15:00: Stop #8: Assateague Island Lighthouse

15:00 – 15:30: Stop #9: Chincoteague National Wildlife Refuge Visitor Center (restrooms)

15:30 – 17:00: Stop #10: Assateague Island beach and trails (vehicle trip and walking)

17:00 – 18:00: Transit back to Chincoteague and free time in "downtown" Chincoteague

18:00 – 19:30: Group Dinner (Don's Seafood Market & Restaurant)

19:30 – 20:00: Return to Chincoteague Bay Field Station

DAY #3: SUNDAY, 22 MARCH 2026

MAINLAND EASTERN SHORE OF VIRGINIA AND THE SAVAGE NECK SAND DUNES

06:30 – 08:00: Breakfast (Chincoteague Bay Field Station Cafeteria)

08:30 – 09:00: Pack and depart Chincoteague Bay Field Station

09:00 – 09:45: Transit to VIMS Eastern Shore Lab (40 Atlantic Ave., Wachapreague, VA)

09:45 – 10:45: Stop #11: Overview of VIMS Eastern Shore Laboratory (ESL) and geologic history of mainland Eastern Shore of Virginia (restrooms)

10:45 – 11:30: Transit to Savage Neck Sand Dunes Natural Area Preserve
Park at Northampton County Administrative Building (16404 Courthouse Road, Eastville) and carpool to site

11:30 – 13:00: Stop #12: Dunes of the Holocene and erosion management in the Anthropocene: Savage Neck Sand Dunes and Beach

13:00: End of conference; depart
Suggested lunch locations: Cape Charles; Virginia Beach
Suggested quick stop (gas, restroom): Royal Farms, 29214 Charles M Lankford Jr Memorial Hwy, Cape Charles

FOREWORD

The text and figures included in this guide are derived from the outcomes of approximately a dozen years of study of the Eastern Shore of Virginia and its barrier islands by scientists, students, and collaborators of the Coastal Geology Lab at the Virginia Institute of Marine Science (VIMS), along with the work of many researchers who came before. The VIMS Eastern Shore Lab (ESL; Wachapreague, VA) played a central role in logistics supporting the vast majority of the field data presented here. We also thank the numerous private homeowners and businesses, the Town of Chincoteague, the National Aeronautics and Space Administration (NASA) Wallops Flight Facility (Shari Miller, Matthew Lindsey, and others), and the Chincoteague National Wildlife Refuge (Kevin Holcomb) for access during this field trip; and Claire Teachey of the Chincoteague Bay Field Station for program and logistical support. Most of the data and work presented here is published, and text is largely derived from associated peer-reviewed publications. Readers are encouraged to explore details in these key resources:

Chincoteague, Assateague and Wallops Islands:

Georgiou, I.Y., Messina, F., Sakib, M.M., Zou, S., Foster-Martinez, M., Bregman, M., Hein, C.J., Fenster, M.S., Shawler, J.L., McPherran, K., Trembanis, A.C., 2023. Hydrodynamics and Sediment-Transport Pathways along a Mixed-Energy Spit-Inlet System: A Modeling Study at Chincoteague Inlet (Virginia, USA), *Journal of Marine Science and Engineering*, v. 11, p. 1075.

Mariotti, G., Hein, C.J., 2022. Lag in response of coastal barrier-island retreat to sea-level rise, *Nature Geoscience*, v. 15, p. 633–638.

McBride, R.A., Fenster, M.S., Seminack, C.T., Richardson, T.M., Sepanik, J.M., Hanley, J.T., Bundick, J.A., Tedder, E. (Eds.), Holocene Barrier-Island Geology and Morphodynamics of the Maryland and Virginia Open-Ocean Coasts: Fenwick, Assateague, Chincoteague, Wallops, Cedar, and Parramore Islands, *in:* Brezinski, D.K., Halka, J.P., Ortt, J. (Eds.), *Tripping from the Fall Line: Field Excursions for the GSA Annual Meeting, Baltimore, 2015: Geological Society of America Field Guide 40*, Geological Society of America, Boulder, pp. 310–334.

Robbins, M.G., Shawler, J.L., Hein, C.J., 2022. Contribution of longshore sand exchanges to mesoscale barrier-island behavior: Insights from the Virginia Barrier Islands, U.S. East Coast, *Geomorphology*, v. 403, p. 108163.

Shawler, J.L., Ciarletta, D.J., Connell, J.E., Boggs, B.Q., Lorenzo-Trueba, J., Hein, C.J., 2021a. Relative influence of antecedent topography and sea-level rise on barrier-island migration, *Sedimentology*, v. 68, p. 639–669.

Shawler, J.L., Hein, C.J., Obara, C.A., Robbins, M.G., Hout, S., Fenster, M.S., 2021b. The effect of coastal landform development on decadal- to millennial-scale longshore sediment fluxes: Evidence from the Holocene evolution of the central mid-Atlantic coast, USA, *Quaternary Science Reviews*, v. 267, p. 107096.

Shawler, J.L., Hein, C.J., Georgiou, I.Y., Messina, F., Sakib, M.M., 2025. Local versus regional controls on the morphology and texture of preserved beach and foredune ridges, *Journal of Geophysical Research: Earth Surface,* v. 130, p. e2025JF008429

Eastern Shore of Virginia Mainland and Savage Neck:

Cahoon, K.M., Hein, C.J., Fenster, M., Clarke, C., Ramsey, K.W., 2025. Updated stratigraphic mapping reveals insights into the late Pleistocene evolutionary history of the Virginia Eastern Shore, US Mid-Atlantic Coast, *Stratigraphy*, v. 22(2), p. 99–134.

Cahoon, K.M., Hein, C.J., Fenster, M.S., Huot, S., 2026. Refined Late-Pleistocene Evolutionary and Sea-Level History for the Delmarva Peninsula, US Mid-Atlantic Coast, *Marine Geology* (in press as of this writing).

Davis, E.H., 2020. A Reassessment of the Late Quaternary Surficial Geology of the Lower Delmarva Peninsula, Virginia. MSc Thesis: University of Delaware, 107 p.

BACKGROUND

Field Trip Geologic and Coastal Setting

This field trip will take us across the Eastern Shore of Virginia (ESVA), from developed and undeveloped barrier islands on the northern "seaside" of the Shore, and to a site of spectacular beach and dunes on its southern "bayside". The ESVA is located along the southern Delmarva (Delaware, Maryland, and Virginia) Peninsula of the U.S. Mid-Atlantic Bight, extending approximately 300 kilometers (km) between the mouths of Delaware and Chesapeake bays (Fig. 1). The Peninsula ranges in width from 110 km in Delaware and Maryland to less than 24 km along the ESVA, and is comprised of preserved depositional and erosional coastal sedimentary features—such as beaches, beach- and foredune-ridge plains, prograding spits, paleo river valleys, wave-cut scarps, and ravinement surfaces (Mixon, 1985; Mixon et al., 1989; Swift et al., 2003; Brothers et al., 2020; Cahoon et al., 2025). The ESVA is characterized by a topographic high along a central spine that runs roughly along the center of the peninsula (Fig. 1b), with elevations generally decreasing to both the east and west.

Tides along the southern Delmarva Peninsula are semi-diurnal. Based on records from 1978 to 2015 Common Era (CE), two local tide gauges recorded mean tidal ranges of 1.23 m (Wachapreague, VA) and 0.64 m (Ocean City, MD; Fenster and McBride, 2015). Local wave data from 1980 to 2012 CE indicate dominant offshore wave heights of 1.2 m and mean wave periods of 8.3 seconds near Assateague Island (Fenster and McBride, 2015). Mean wave heights decrease to the south to ~0.95 m along the southern ESVA (Fenster and McBride, 2015). Dominant winds are from the north (associated with the passage of extratropical northeast storms), leading to net southerly longshore transport (Wright et al., 1986; Fenster et al., 2016). Hayden (2003) documents a gradual increase in the frequency of storm cyclone impacts along the ESVA between 1885 and 2002, with notable periods of reduced storminess in the 1940s and 1970/1980s. However, Dominguez et al. (2024) found no statistically significant increase in storm frequency, but a modest statistically significant increase in storm magnitude between 1927 and 2022 in this region.

Recorded sea-level rise rates of 3.60–6.02 mm yr^{-1} (King et al., 2011; Sallenger et al., 2012; Boon and Mitchell, 2015; Fenster and Bundick, 2015) in the vicinity of Wallops Island are 2.5–5.9 times higher than the long-term rate of global mean sea-level rise (*i.e.*, 1.4 mm yr^{-1}; 1901–2010; IPCC 2014) and 1.1–1.9 times greater than the short-term rate of global sea-level rise (3.2 mm yr^{-1}; 1993–2010; IPCC 2014).

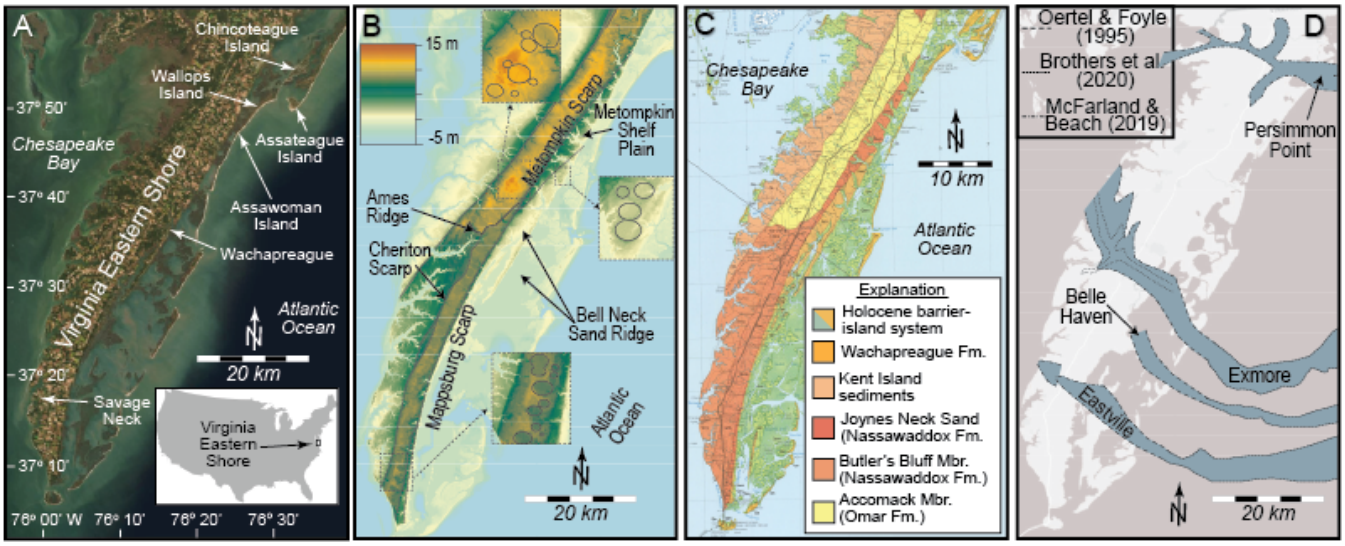

Figure 1. Eastern Shore of Virginia (ESVA). Displayed are (a) a satellite image showing major field locations for this trip; (b) topography of the Shore (digital elevation model by Faunce and Rapp [2020]; scarps and marine terrace locations from Mixon [1985]); (c) surficial geologic map of the ESVA (cropped from Virginia Coastal Plain map of Mixon et al. [1989]); and (d) positions of buried paleochannels as identified by McFarland and Beach (2019; mainland), Oertel and Foyle (1995, backbarrier), and Brothers et al. (2020; offshore). Modified from Cahoon et al. (2025).

Brief Pleistocene Geologic History of the Mainland Eastern Shore of Virginia

The ESVA is built atop mid-Pliocene (3.3–3.2 megaannum [Ma]) coastal, nearshore, and shallow shelf deposits stretching from the Piedmont/Coastal Plain boundary to the modern continental shelf (Mixon, 1985; McFarland and Beach, 2019; Dowsett et al., 2021). The ESVA formed and grew through extension via progressive welding and alongshore elongation of transgressive barrier-island and spit systems along its eastern ("seaside") and western ("bayside") margins during successive Pleistocene relative sea-level highstands (Mixon, 1985; Oertel and Overman, 2004; Krantz et al., 2016; McFarland and Beach, 2019). Sediments were largely sourced from rivers draining the Piedmont and interior highlands of eastern North America; the filled paleo-valleys of these rivers remain preserved under the ESVA (Colman et al., 1990) and as a broad offshore network of paleochannels (Brothers et al., 2020).

Periods of highstand (interstadials) and lowstand (stadials) during the last glacial period are commonly referred to by their Marine Isotope Stage (MIS), a system in which alternating warm (odd numbers) and cold (even numbers) paleoclimate periods, as derived from oxygen isotope ($\delta^{18}O$) data in deep-sea core samples. Marine Isotope Stage 1 represents the current interglacial (Holocene), with higher numbers referring to older stadial, interstadial, and interglacial periods, often subdivided by letters (*e.g.*, 5a–5e). Figure 2 provides a timeline of MIS relevant to the formation of most of the ESVA, those since the last interglacial (MIS 5e, 125,000 years ago). The units on the ESVA which are generally attributed to this latter Pleistocene period are (from oldest to youngest; Fig. 1c): the central Accomack Member (Mbr.) of the Omar Formation (Fm.) (pre-MIS 5e, likely the MIS 7 or 9 interglacial), the Joynes Neck Sand (MIS 5e), Onancock Mbr. (bayside) and the Butlers Bluff Mbr. (seaside) of the Nassawadox Fm. (MIS 5e and 5c), and the Kent Island sediments (bayside) and Wachapreague Fm. (seaside) (MIS 5a) (Mixon, 1985; McFarland and Beach, 2019). The latter was recently formally differentiated into the Locustville and Upshur Neck Mbrs. (Cahoon et al., 2025), likely each associated with separate highstands of relative sea level (Cahoon et al., 2026).

In general, these units are oriented roughly parallel to the modern shoreline (north-northeast to south-southwest) and bounded by scarps (Kiptopeake, Cheriton, Pungoteague, Ames Ridge, Mappsburg, Metompkin, Oak Hall, and Temperanceville; Mixon, 1985). These units were formed as a series of shallow-water and subaerial coastal units which were deposited during sequential periods of sea-level highstand during the last-interglacial/glacial cycle. They fill and overlie ancestral paleochannels carved during sequential lowstands throughout the early to mid-Pleistocene (Swift et al., 2003; McFarland and Beach, 2019; Brothers et al., 2020), or were emplaced directly atop the Yorktown and Chowan River formations, which are shallow shelf sediments deposited during the mid-Pliocene (Ward and Blackwelder, 1980; McFarland and Beach, 2019; Dowsett et al., 2021). These mainland geologic units extend eastward offshore, where they are lumped as seismic unit "Q2" by Brothers et al. (2020) and Wei and Miselis (2023) and northward into Maryland and Delaware where they are correlated with the Ironshire and Sinepuxent formations (Owens and Denny, 1979; Ramsey, 2010; Cahoon et al., 2025). On land, all are at least partially covered by aeolian sand deposits originating from subaerial erosion and remobilization of earlier coastal deposits during colder stadials (Lowery et al., 2010; Cahoon et al., 2025).

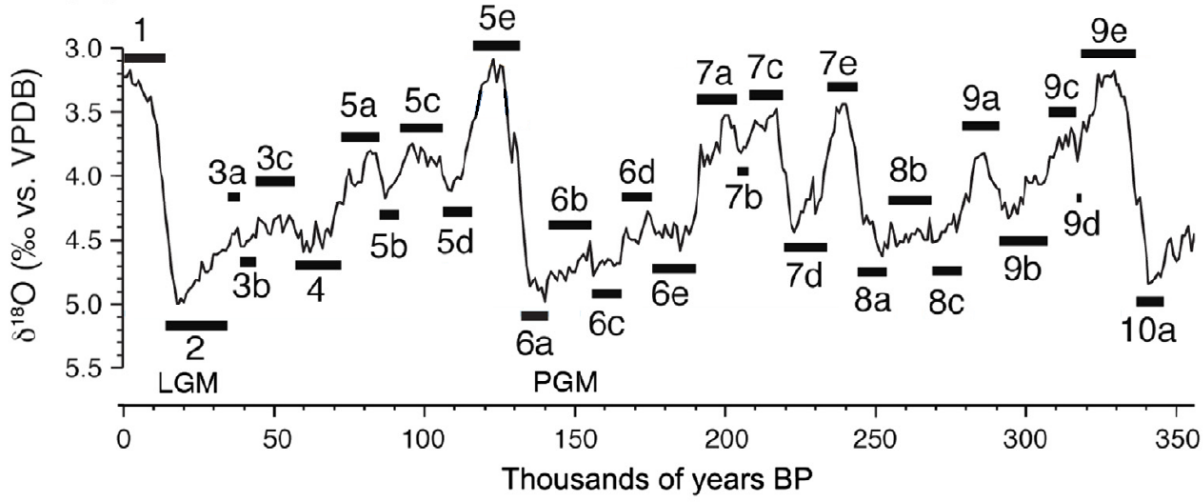

Figure 2. Marine Isotope Stages (MIS) of the last 350,000 years. Figure modified from Railsback et al. (2015) and Pickering et al. (2018). Most of the exposed landscape of the Eastern Shore of Virginia formed since MIS 5e, with only the Accomack Member likely predating that last interglacial at ~125 kiloannum (ka). BP = Before Present (1950 CE); LGM = Last Glacial Maximum; PGM = Penultimate Glacial Maximum; VPDB = Vienna Pee Dee Belemnite (international standard for oxygen isotope ratios).

The Holocene Virginia Barrier Islands

Most of the Delmarva Peninsula is bordered to the east by a complex of low-lying barrier islands, broad tidal lagoons, and salt marsh (Fig. 3). These islands first formed >5000 years ago, several kilometers offshore of their current positions, and gradually migrated landward (Finkelstein and Ferland, 1987; Raff et al., 2018). A number of studies have demonstrated the dynamism of the Virginia Barrier Island chain, or of individual islands within the chain, since the 19th century (Rice et al., 1976; Dolan et al., 1979; Leatherman et al., 1982; Rice and Leatherman, 1983; Oertel et al., 1989; Pendleton et al., 2004; Fenster and Hayden, 2007; Richardson and McBride, 2007, 2011; Psuty and Silveira, 2011; Nebel et al., 2012; Richardson, 2012; Hapke et al., 2013; Walters et al., 2014; Deaton et al., 2017; Raff et al., 2018; Hein et al., 2019; Shawler et al., 2021a,b; Mariotti and Hein, 2022; Robbins et al., 2022; Shawler et al., 2025).

At the northern end of this chain is Assateague, a 60-km long, wave-dominated barrier island. The southern ~10 km of this island is characterized by rapid elongation since the early 1800s and growth of the Tom's Cove Isthmus spit neck and "Fishing Point" spit hook (Hein et al., 2019). Islands south of Assateague are 3–12 km long, 0.1–1.0 km wide, located 2.0–13.5 km offshore, and are classified as mixed-energy (*sensu* Hayes, 1979). They are backed by varying amounts of salt marshes, tidal flats, and shallow (1–2 m) open-water bays. Presently under a mixture of private, federal (U.S. Fish and Wildlife Service, National Aeronautics and Space Administration, U.S. National Parks Service, U.S. Department of Defense), state (Virginia Department of Conservation and Recreation), and non-governmental organization (The Nature Conservancy) ownership, these barrier islands have largely been undeveloped since the early 1900s, and most have never undergone any large-scale shoreline stabilization (Barnes and Truitt, 1997). The only exception is Wallops Island, where approximately 4.5 km of the shoreline has been partially hardened since the mid-1900s and nourished three times, in 2012, 2014, and 2021 (Fenster and Bundick, 2015; Elko et al., 2021). This island chain, extending to Fishermans Island, located at the northern mouth of Chesapeake Bay (Fig. 3), has generally been classified into three categories according to the modes of shoreline retreat of individual islands: (1) a northern group (Wallops, Assawoman, Metompkin, Cedar) characterized by shore-parallel retreat; (2) a central rotational group (Parramore, Hog, Cobb) characterized by classic "drumstick" morphology in which one end of these wide, dune-filled and highly vegetated barriers is notably wider than the other; and (3) a southern group (Wreck, Ship Shoal, Myrtle, Smith) characterized by landward migration in a manner non-parallel to the mainland shoreline (Leatherman et al., 1982; Kochel et al., 1985). However, all but Wallops and

Fisherman's islands are rapidly transgressing through either island narrowing (erosion) or wholesale landward migration (Fig. 3). This has led to accelerating exposure of backbarrier salt marsh along the beach and upper shoreface, leading to loss of >30 km^2 of salt marsh since the mid-1800s (Deaton et al., 2017) and 26.1 gigagrams of peat and lagoon organic "blue carbon" stores annually (Barksdale et al., 2023). Coastal change along this stretch is so rapid that several islands show evidence of transitioning beyond their traditionally classified behaviors. For example, Parramore Island, classified as "rotational", has largely undergone parallel beach retreat during the last several decades (Raff et al., 2018). Cobb Island likewise has fully transitioned to nonparallel retreat over historical time, and in the past decade has breached to form two "permanent" islands. As of 2025, Hog Island is the only considered to show evidence of rotational instability.

One possible explanation for these accelerating transitions is sand sequestration on the ebb deltas of several of the tidal inlets along this reach (Fenster and FitzGerald, 2014). This process may be a response to an increase in inlet tidal prisms resulting from a long-term decline in backbarrier marsh, potentially signaling a state transition to what has been termed "runaway transgression" (FitzGerald et al., 2008) . However, if runaway transgression is active in this system, the processes sustaining ebb-tidal sand sequestration may be overwhelmed by the very rapid (4.8 m yr^{-1}, 1980–2017 CE; Mariotti and Hein, 2022) landward migration of these barriers, which leads to a gradual loss of backbarrier area and decreasing tidal prism (Deaton et al., 2017; FitzGerald et al., 2018).

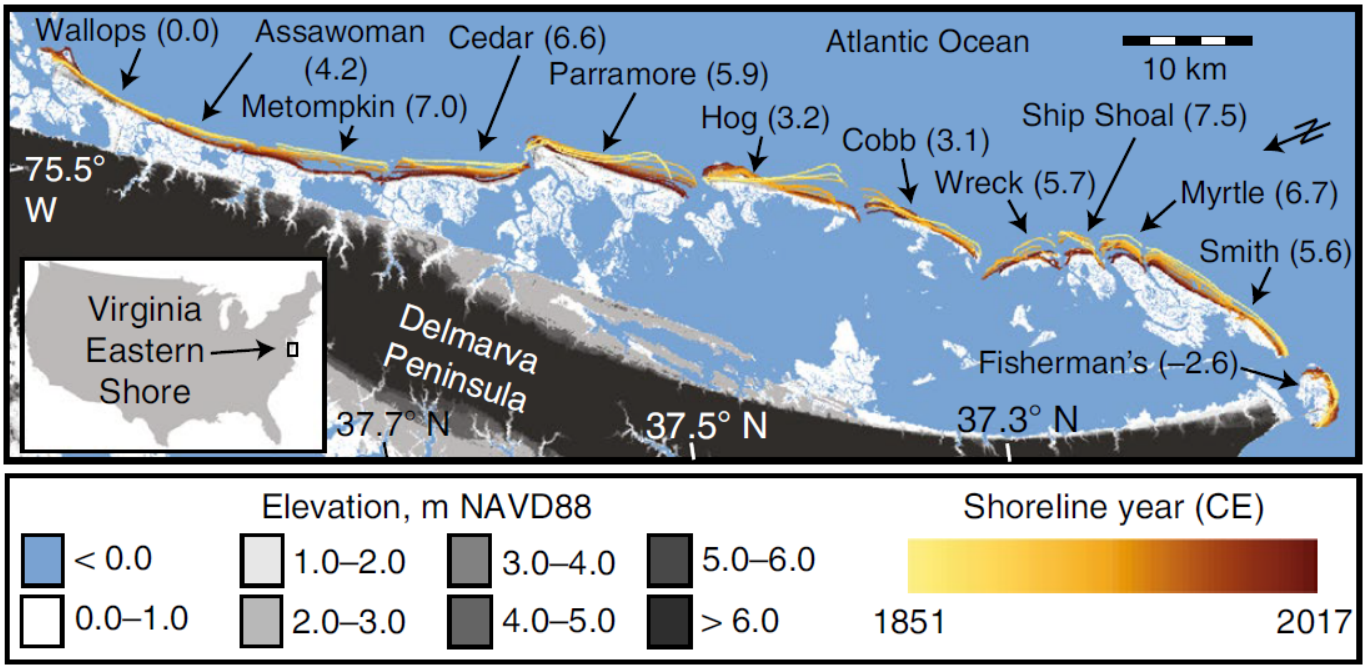

Figure 3. Historical shoreline changes along the Virginia Barrier Islands, 1851–2017 CE. Background digital elevation model is derived from 2016 Lidar (US Geological Survey). Numbers in parentheses following island names are average island-wide shoreline change rates for 1851–2017 in units of m yr^{-1}. Modified from Mariotti and Hein (2022).

CONFERENCE DAY #1: THE CHINCOTEAGUE BAY FIELD STATION

The March 2026 Virginia Geological Field Conference is being hosted at the Chincoteague Bay Field Station (CBFS), a coastal environmental education center dedicated to hands-on learning in marine science, ecology, and coastal sustainability. CBFS provides access to a variety of ecosystems, including salt marshes, barrier islands, tidal flats, and maritime forests, while also serving a wide range of audiences, including college students, K–12 school groups, teachers, and families. Its college-level programs provide field-based, experiential-learning courses in marine biology, oceanography, environmental science, and related disciplines. For younger students, CBFS runs school programs, summer camps, and home-school days focused on science education and environmental stewardship, and involve activities such as seining, kayaking, specimen collection, and habitat exploration. In addition to education, CBFS also supports research and teacher professional development, helping educators integrate field science into their curricula.

CONFERENCE DAY #2: THE NORTHERN VIRGINIA BARRIER ISLANDS ASSAWOMAN, WALLOPS, CHINCOTEAGUE, AND ASSATEAGUE ISLANDS

The Assateague-Chincoteague-Wallops-Assawoman system is situated at the north-to-south transition from long, linear, wave-dominated barrier islands of southern Delaware and Maryland, to the shorter, mixed-energy Virginia Barrier Islands. This multi-barrier system is dominated by Chincoteague Inlet, which is the largest and arguably the most dynamic tidal inlet along the Delmarva Peninsula. Over the course of the day, we will start at the southern-most barriers in this system. One of these barriers, Assawoman, is essentially in its "natural" state, while the other (Wallops) is heavily managed. Next, we will work our way north to the now "relict" barrier island of Chincoteague and finally to the rapidly elongating island of Assateague. Saturday's field stops are shown in Figure 4.

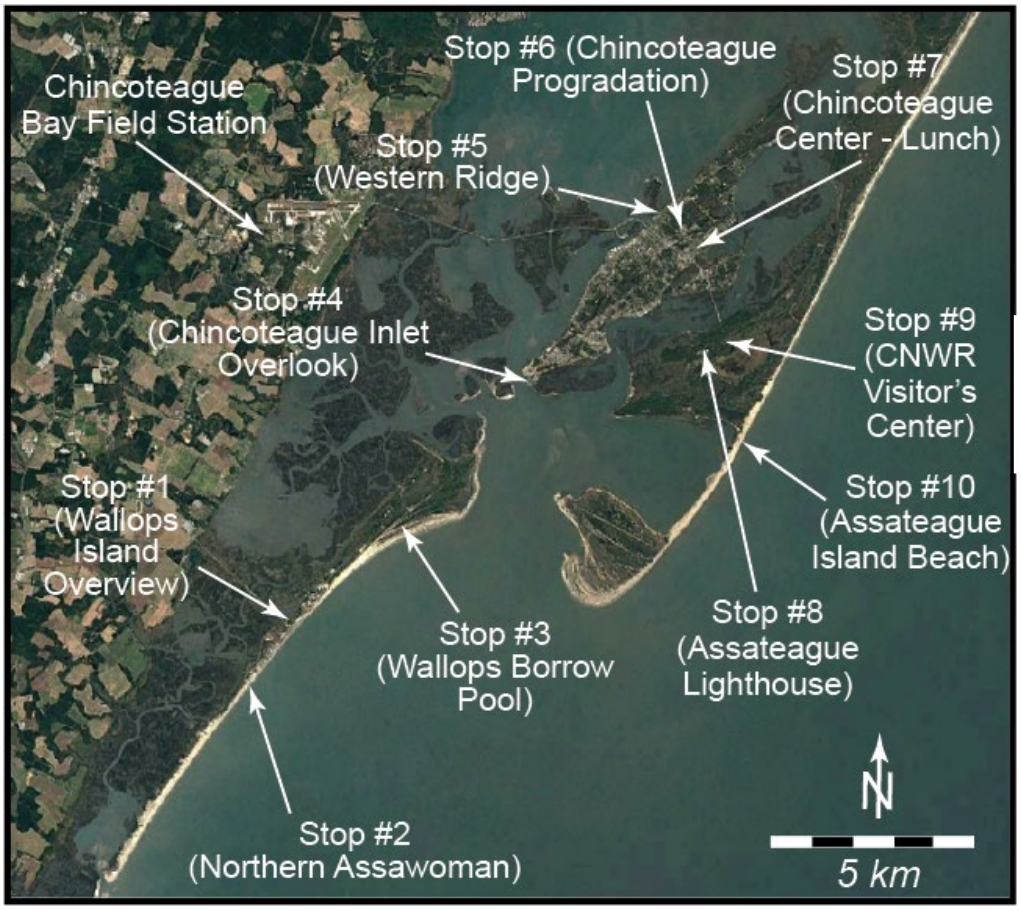

Figure 4. Saturday field stops.

SATURDAY MORNING: BACKGROUND

Our first stops on Saturday morning will bring us to Wallops and Assawoman islands. Located south and west of Chincoteague Inlet, Wallops and Assawoman are presently conjoined, forming a continuous stretch of beach and dunes >15 km long. Wallops is largely comprised of sandy beach, vegetated low-lying dunes, patches of dense shrubs, tidal pools, and creeks, with sand flats and peat banks on the northern tip of the island. Assawoman is 4 km long, one quarter of which is beach habitat and the remainder contains extensive salt marshes. These islands are backed by salt marsh, tidal creeks, and bays. Wallops is characterized by a bulbous northern end (~1500 m wide) comprised of a series of arcuate beach and foredune ridges oriented southwest-northeast, most of which formed during the late 20th and early 21st centuries (Shawler et al., 2021b). To the south, Wallops narrows to only ~300 m wide. An inlet separating Wallops Island from Assawoman Island closed in the mid-1960s in response to an engineered reduction in tidal prism, essentially negating the need for water to transit between the backbarrier and coastal ocean through this inlet (Fenster and Bundick, 2015).

Between 1851 and 2017 the combined Wallops-Assawoman Island experienced a net increase in volume of 10.5×10^6 m^3 (+51%; 530,000 dump trucks worth of sand, roughly a line of them stretching bumper-to-bumper from Washington DC to New York City) at a rate of 6.3×10^4 m^3 yr^{-1} (Robbins et al., 2022). These islands increased in volume between 1851 and 1908, then decreased between 1908 and 1962. From 1962 to 2017, they experienced steady linear growth, largely in response to progradation and modest elongation of Wallops Island north of the nodal zone created by the wave shadow of Fishing Point (Shawler et al., 2021b; Robbins et al., 2022); this nodal zone is the site of our first stop.

STOP #1: WALLOPS ISLAND CAMERA TOWER

Since 1945, the National Advisory Committee for Aeronautics and its successor, NASA, has owned and managed Wallops Island. The island also houses infrastructure of the U.S. Navy and Virginia Spaceport Authority's Mid-Atlantic Regional Spaceport. The need to protect associated infrastructure has resulted in a complex series of shoreline stabilization activities over the past ~80 years (Table 1).

Our first stop provides a nice overview of some of the measures put into place. Specifically, immediately at the foot of the camera tower sits a large rip-rap revetment (seawall) constructed, in several phases, along >2 km of the Wallops shoreline (Table 1). Step up onto the tower and you can see a pair of rubble mound breakwaters to the north, and in the distance to the south a set of three additional breakwaters. These were constructed in 2020–2021 in response to ongoing erosion and undercutting of the seawall. Coincident with installation of these breakwaters was the extraction of >841,000 m^3 of sand from northern Wallops (the borrow site is stop #3), which was used to assist with breakwater construction and to nourish the beach along this stretch of the island (Alvino et al., 2025). The beach was extended seaward by >100 m at the site of each breakwater, allowing for delivery of rocks to build the breakwaters from the mainland (as opposed to barging them in, as would be done in lower-energy environments such as Chesapeake Bay). This sand was later removed, leaving detached breakwaters fronting shoreline protrusions known as "salients". The breakwaters did their job however, trapping sand behind them and allowing the beach to build back out. Some of the breakwaters have reconnected to the beach in the form of what coastal geologists call "tombolos". Steady erosion of the beach seaward of the revetment between the breakwaters over the past several years has left little sand exposed along much of the stretch, even at mid and low tide. Plans are underway (under review with the Coastal Zone Management Program as of this writing in February 2026, with permit applications submitted to the Virginia Marine Resources Commission shortly) for construction of additional breakwaters sets and beach nourishment (this time from an offshore shoal) to continue to strengthen this shoreline against ongoing erosion.

Table 1. History of beach stabilization measures on Wallops Island, Virginia. Modified from Alvino et al. (2025), with original data from NASA (2010), King et al. (2011), NASA (2019), and USACE (2018).

Year	Shoreline Stabilization Activity
1945	National Advisory Committee on Aeronautics (NACA, now NASA) started using Wallops Island as rocket launch site. 1st seawall constructed out of steel sheet pile; expanded through the 1980s.
1946	U.S. Army Corps of Engineers Beach Erosion Board recommends installation of wooden groins. By 1972 47 wooden groins had been constructed, but did little to prevent erosion and had largely degraded by the mid-1980s.
1959	Construction of the causeway to Wallops Island and installation of the first wooden groins.
1962	Ash Wednesday Storm (March) causes a breach on the southern end of Wallops, which was subsequently mechanically filled with sand.
1988	Installation of sand retention units ("beach prisms"); largely unsuccessful.
1992	Sheet pile seawall (in disrepair) was replaced with 4,840 m of rip-rap revetment.
2007	Emergency placement of temporary geotextile tubes on the beach south of the seawall.
2009	Impact of large November storm which causes substantial island flooding and damage to the geotextile tubes.
2010	Wallops Flight Facility Shoreline Restoration and Infrastructure Protection Program formed. First Environmental Impact Statement was finalized (fieldtrip guide coauthor M. Fenster was an author). Recommended extension of the rip-rap revetment by 1,400 m and beach nourishment every 3–7 years (average volume: 616,000 m^3) every 5 years over a 50-year span.
2011	Construction of initial 435 m seawall expansion (August 2011 – March 2012). Storm Damage Reduction Project Design (King et al., 2011) report completed and published.
2012	Beach renourishment along 6,000 m of shoreline (April – August). Sediment taken from an offshore borrow site. In October, Hurricane Sandy made landfall, damaging the seawall and southern two-thirds of the renourished beach.
2014	Repairs to seawall and beach renourishment (July – September).
2015	Landfall of Hurricane Joaquin, with attendant heavy erosion along Wallops.
2016	Landfall of Winter Storm Jonas. Combined loss from Joaquin and Jonas: 775,516 m^3.
2018	Landfall of Winter Storm Riley caused additional reduction in sand volume on Wallops.
2020–2021	Construction of five breakwaters backfilled with 841,010 m^3 of sand extracted from northern Wallops Island beach (April 2020 – April 2021).

Sediment Transport Dynamics Along the Wallops Island Nodal Zone

Erosion dominates this stretch of Wallops Island for multiple reasons, including sea-level rise, complex wave refraction processes around southern Assateague Island during northeast storms, and an overall dearth of sand in the nearshore and along beaches south of Assateague; the latter is linked to growth of Assateague Island, which is something we will cover later in the day. The role of these background drivers is evident in the behavior of the barrier chain overall, with nearly every barrier island (except southern Assateague, northern Wallops, and Fisherman's Island) experiencing rapid transgression via erosion (island area loss) and/or landward island migration, with shoreline migration rates reaching a system-wide rate of ~3.3 ± 0.3 m yr^{-1} from 1851 to 1933 accelerating to ~4.8 m yr^{-1} from 1980 to 2017 (Fig. 3). This shoreline transgression is largely due to erosion: the Virginia Barrier Islands have experienced a net overall sand loss of ~28×10^6 m^3 since the middle to late 1800s (Robbins et al., 2022),

and rates are poised to accelerate into the future as lagging shoreline change catches up to ever-accelerating sea-level rise (Mariotti and Hein, 2022).

Of all the islands, central Wallops Island is in a particularly precarious position, due to the configuration of the adjacent barrier chain. Southern elongation of Fishing Point (Assateague Island) since the mid-1800s has not only trapped sand, but likely also influenced longshore sand delivery rates by altering downdrift transport gradients (Robbins et al., 2022; Shawler et al., 2025). Waves approaching at an angle to the coast create gradients in alongshore sediment flux, and lead to self-organizing accretionary sand waves and spits, and downdrift erosional hotspots within the associated wave shadow (Thomas et al., 2016; Murray et al., 2020). This process was described in detail for Fishing Point by Jones (2016). In short, refraction of dominant northeast storm waves around Fishing Point creates a nodal zone along downdrift Wallops Island, from which dominant longshore transport diverges to the north and south at a maximum rate of ~4.6×10^4 m^3 yr^{-1} (King et al., 2011; Fenster and Bundick, 2015). One direct effect is the accumulation of ~7.3×10^6 m^3 of sand along the northern 4 km of Wallops Island, resulting in ~500–1500 m of net progradation since the mid-1800s. Within the nodal zone—located approximately within the area of Wallops bounded by the breakwaters—net transport is near zero, but it gradually increases to the north and south with distance from south-central Wallops Island. This creates a transport gradient in which the southern ends of islands south of the nodal zone experience higher rates of southerly transport than the northern ends. This imbalance leads to net sand export away from central Wallops Island (Fig. 5), allowing for rapid growth of northern Wallops and impacts felt 10 or more kilometers to the south (Jones, 2016).

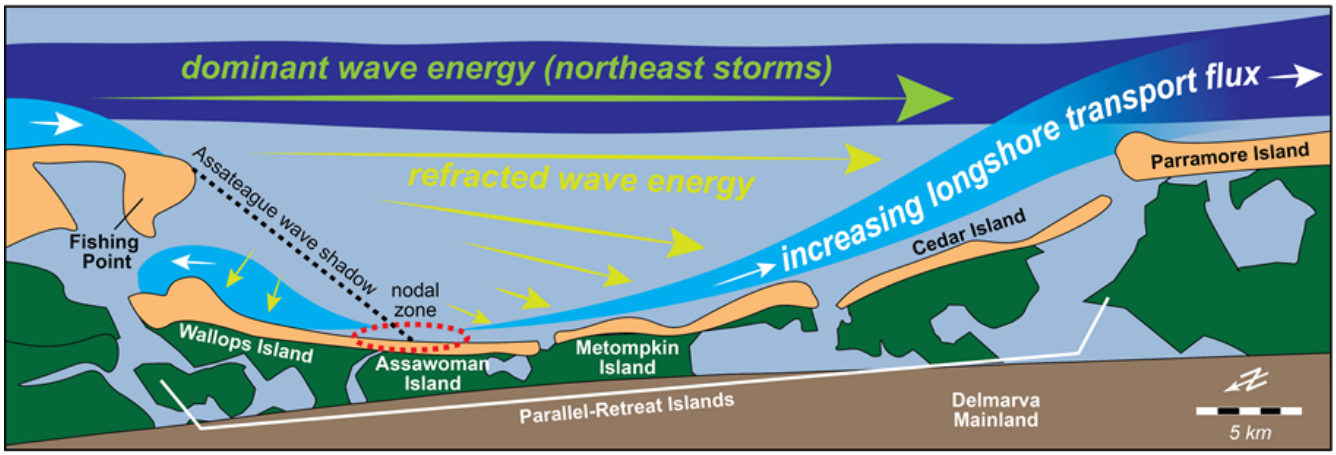

Figure 5. Conceptual model of the role of Fishing Point (southern Assateague Island) in causing a wave shadow south of Assateague, nodal zone along central Wallops Island (with associated reversal of longshore transport towards northern Wallops), and a downdrift-propagating longshore transport gradient south of the nodal zone. From Robbins et al. (2022).

Science to Inform Management: Ongoing Coastal Geological Study of Wallops Island

The VIMS Coastal Geology Lab, along with partners at the Virginia Department of Wildlife Resources, Virginia Tech, The Water Institute, the U.S. Geological Survey, the University of Delaware, and Randolph-Macon College (collectively, "coastal physical processes team") are currently undergoing a multi-year mapping and monitoring effort of Wallops and Assawoman islands, to provide information to assist NASA with future stabilization efforts (NASA, 2024). The project scope focuses on collecting shoreline-change, sediment-volume, abundance (or counts) and distribution of federally listed species, and habitat-area-change data at high temporal and spatial resolution along Wallops Island and backbarrier habitats. This study allows for mapping of beach and nearshore habitat recovery from disturbance activities (sand extraction, breakwater construction, beach nourishment); monitoring of stabilization project efficacy; and assessment of stabilization project impacts on Wallops Island beach and nearshore habitats located outside of the project footprint. The existing Chincoteague Inlet Modeling Study (CIMS) model, developed by a VIMS- and Water Institute-led team in collaboration with the Town of Chincoteague, is being refined through integration of high-resolution bottom mapping (bathymetry, sediment

sampling) and oceanographic process data to be collected as part of this study. Scenario testing using this model supports ongoing and future management activities, will aid in monitoring and assessment efforts, and bolster long-term resilience planning.

The coastal physical processes team is collecting, over the course of five years (2024–2029): (1) seasonal beach and nearshore sediment samples for textural analysis along 25 cross-shore transects, along with real-time kinematic Global Positioning System (RTK-GPS) topographic and multibeam bathymetric data on these same transects (Fig. 6); (2) full swath topography along Wallops and Assawoman islands using unmanned aerial system (UAS) based photogrammetry; (3) high-resolution bathymetric and sediment textural data on the nearshore and lower shoreface (Fig. 7); and (4) monthly, remote-sensing-based shoreline-change mapping to reveal trends in beach behavior in response to natural conditions and engineering interventions (Fig. 8). These data support development and refinement of engineering scenarios using a numerical hydrodynamic and sediment-transport model (CIMS; Fig. 9), calibrated with new nearshore oceanographic process data.

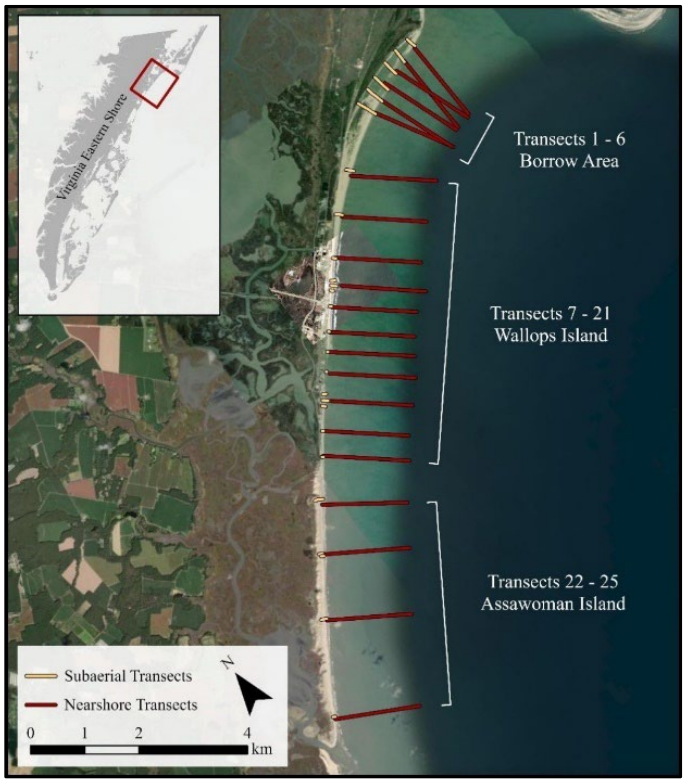

Figure 6. Subaerial and nearshore cross-shore transects across Wallops and Assawoman islands, where topographic, bathymetric, and sediment textural data are being collected as part of a multi-year mapping and monitoring study to inform future management of Wallops Island

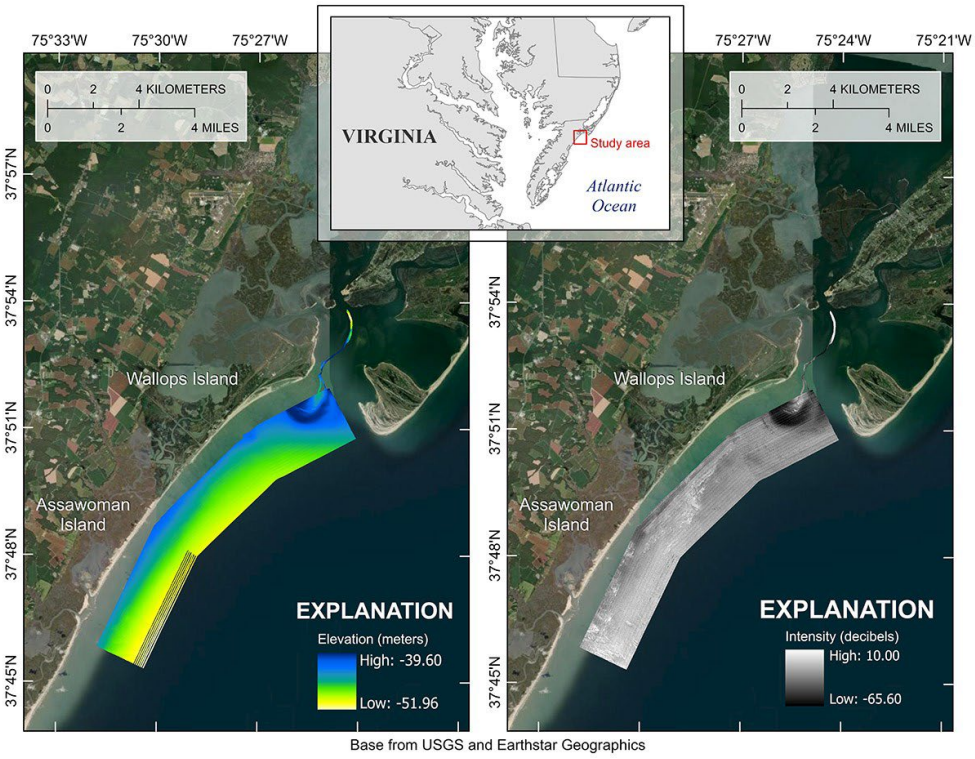

Figure 7. Multibeam bathymetry (left) and backscatter data (right) collected along the shoreface of Wallops and Assawoman Islands in 2024 by the U.S. Geological Survey team as part of the ongoing Wallops Island Shoreline Resiliency Study. Data are represented by a 1-meter digital elevation model in WGS84 (G2139) ellipsoid height, and intensity values are shown in decibels (dB). Figure from Bemelmans et al. (2025)

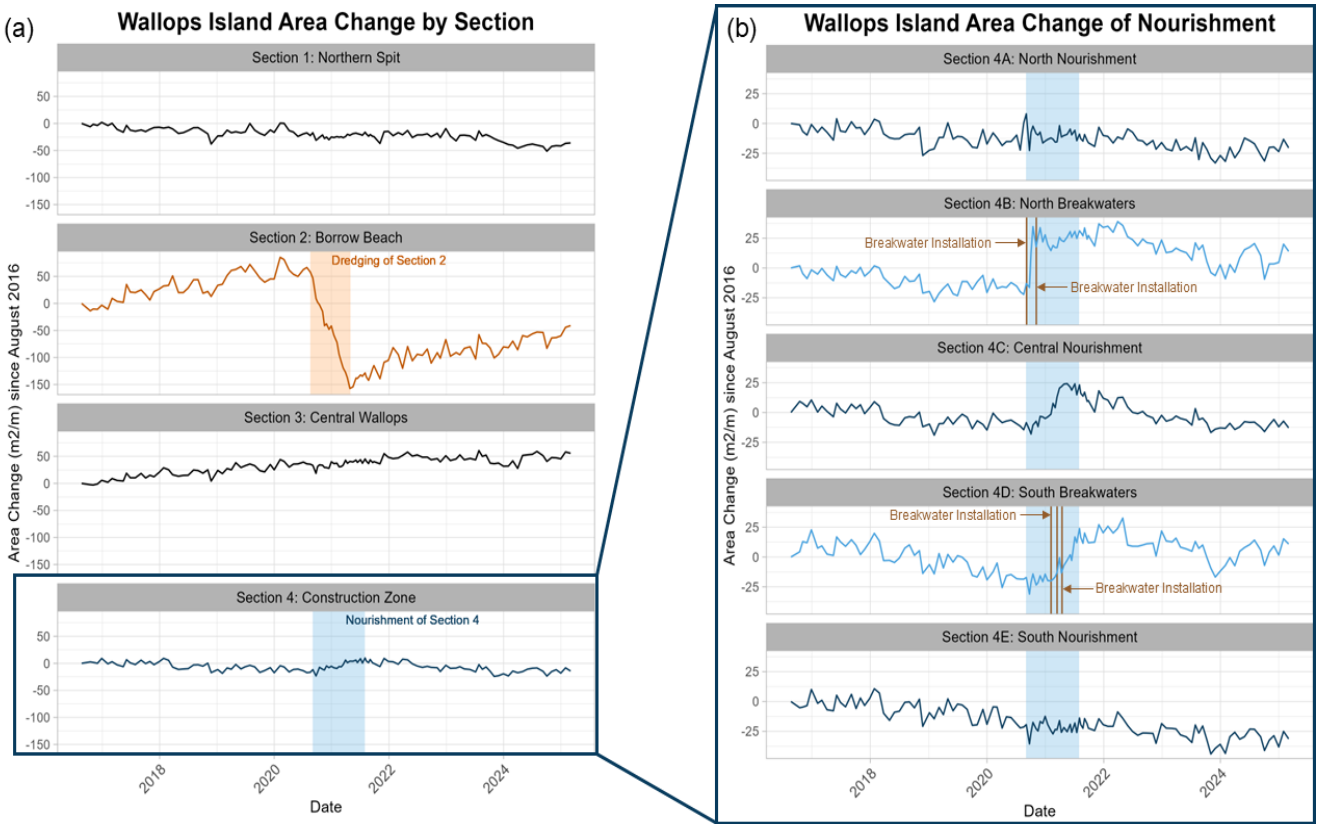

Figure 8. (a) Stacked line graph illustrating area change ($m^2\ m^{-1}$) for Sections 1–4 from August 2016 to March 2025. The orange box indicates Section 2 dredging (estimated August 19, 2020 – April 30, 2021), while the blue box delineates the Section 4 nourishment period (estimated September 1, 2020 – July 31, 2021). (b) Stacked line graph displaying area change for Sections 4A–4E. The blue boxes indicate the estimated nourishment period. Vertical brown lines in Sections 4B and 4D denote breakwater installation dates.

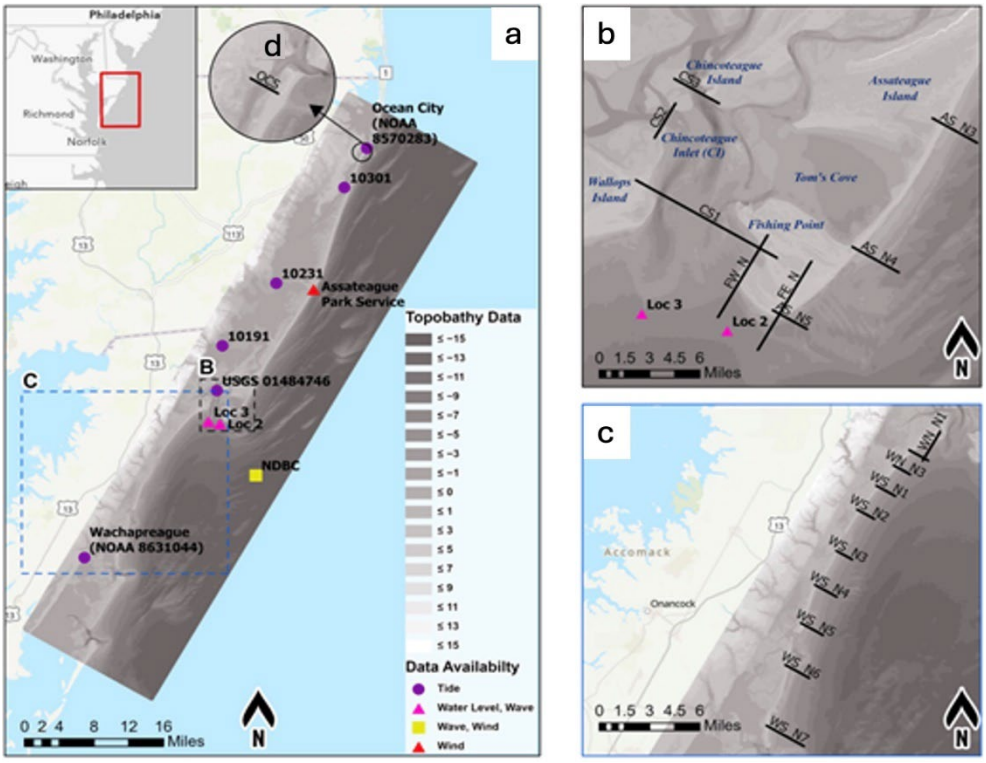

Figure 9. (a) Model region overview topography and bathymetry. Stations shown in (a) and (b) were used to collect wind, wave, and tide data to feed the model. Black lines show in (b) and (c) are cross sections used for discharge and sediment transport analysis. Figure modified from Georgiou et al. (2023).

STOP #2: NORTHERN ASSAWOMAN ISLAND

At this stop we'll park on the road and walk out onto the beach. Looking to the north, you'll see another camera tower and the southern end of the Wallops Island seawall. Approximately 1 km to the north, the three southern breakwaters are visible. Looking to the south, the landscape changes dramatically. In contrast to highly engineered Wallops Island, the Assawoman (southern) portion of this conjoined island is undeveloped and not hardened or nourished. Historically, Assawoman Island has largely migrated landward (west) at a rate of 4.2 m yr^{-1} (Mariotti and Hein, 2022) while maintaining a similar (narrow) width (Robbins et al., 2022; Fig. 10). The geo-morpho-dynamics operating along the northern part of Assawoman Island are characteristic of many of the islands to the south: low in elevation, with discontinuous foredunes, and irregularly spaced washover deposits. The low-lying washover deposits, which are produced by the process of overwash, sit ~1 m above the mean high-water line and make excellent breeding and nesting habitat for the federally endangered piping plover and other migratory shorebirds. These relative topographic lows on the island are susceptible to frequent inundation during the passage of both tropical (e.g., hurricanes) and extratropical (e.g., nor'easters) storms. Although overwash processes are known to be one of dominant forces driving the landward migration of the low-lying islands along the Virginia Barrier Islands (e.g., Shawler et al., 2021a), the exact frequency, magnitude, and duration of overwash events along Assawoman Island is largely unknown. Current work led by contributing author William McCormick (VIMS) includes quantifying how frequently and severely these washover deposits experience overwash to better determine the relative influence of storms on the sediment budget—the relative amount of sediment that has been added or removed from the barrier island—on Assawoman Island. The project uses several Measuring Overwash (or MeOw) stations (Fig. 11), which use ultrasonic distance sensors to record the changes in bed surface elevation along two distinct washover deposits up to every second during storm events. These MeOw stations were deployed in July 2025 and have since collected data during the energetic conditions produced by multiple hurricanes within the Atlantic Ocean.

During the recent passage of Hurricane Erin between 19–23 August 2025, Assawoman Island experienced significant flooding, with water levels on the barrier island interior reaching ~1.5 m above the typical mean high-water line (Fig 11b). The MeOw stations documented six discrete overwash events during this storm, each coinciding with separate high tides (Fig. 11c). These overwash events deposited substantial volumes of sediment on the existing washovers along Assawoman Island, raising the bed surface elevation of the washovers by as much as ~45 cm (preliminary results; pending publication by McCormick et al.). These bed surface elevation changes measured by the MeOw stations will be compared to pre- and post-storm UAS-derived datasets that will allow for quantification of transported sediment volumes, and thus the storm contributions to the sediment budget resulting from Hurricane Erin along Assawoman Island.

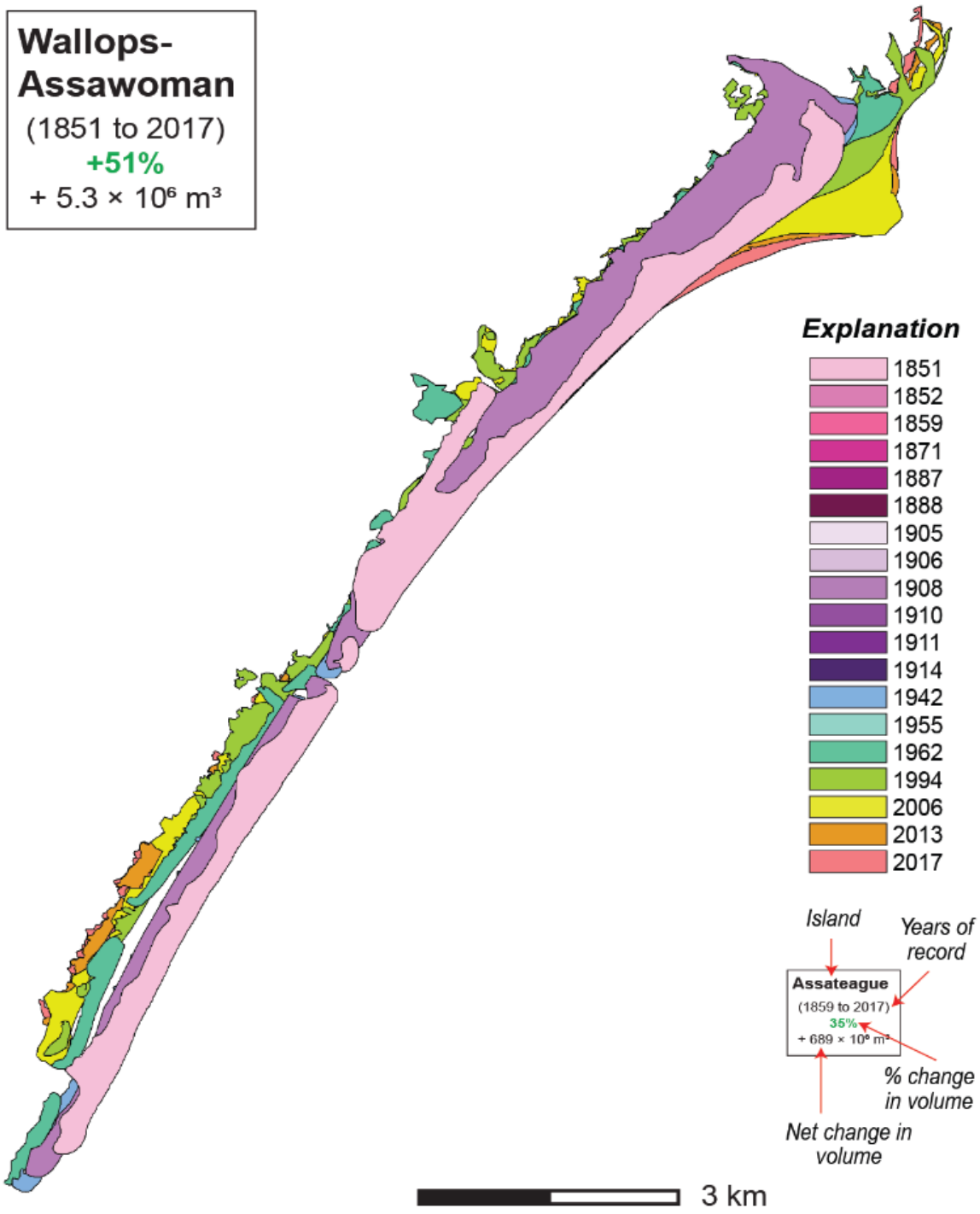

Figure 10. Area and relative position of the Wallops-Assawoman barrier island from the mid-1800s to 2017 CE. Consecutive outlines of each island are overlain at the same scale and in georeferenced relative positions. Modified from Robbins et al. (2022).

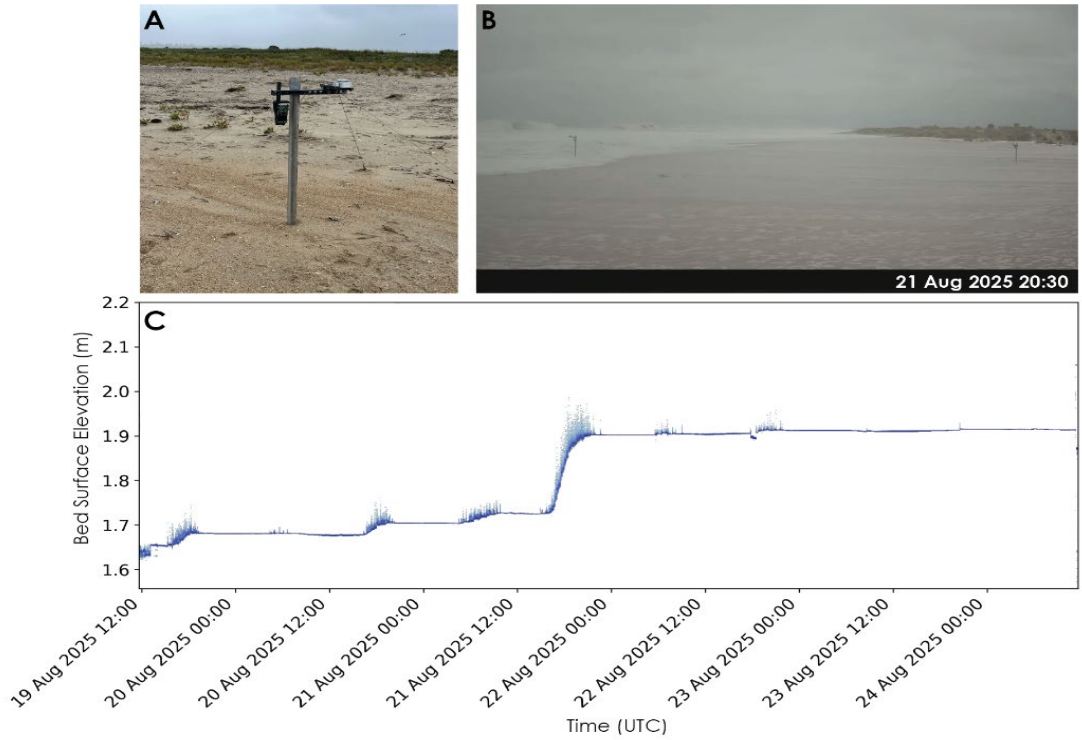

Figure 11. (a) Image of Measuring Overwash (MeOw) station located along Assawoman Island. (b) Photograph showing two MeOw stations measuring water levels during overwash produced by Hurricane Erin in August 2025. (c) Density plot showing the change in bed surface elevation measured by a MeOw station during Hurricane Erin. Note the six occurrences of inundation, which resulted in a total of ~30 cm of aggradation along the washover fan.

STOP #3: NORTHERN WALLOPS AND THE SAND BORROW PIT

Our final stop on Wallops brings us to the rapidly growing, bulbous northern end of the island, which has been prograding in an easterly to southeasterly direction since the late 1800s through the growth of successive wave-built beach and wind-built foredune ridges. Progradation is largely in response to sand delivered from across Chincoteague Inlet and the nodal zone to the south (Georgiou et al., 2023; see Fig. 5). During this time, northern Wallops Island trapped 7 x 10^6 m^3 of sand at an average rate of 42,000 m^3 yr^{-1}. An additional 4.2 x 10^6 m^3 yr^{-1} of mixed sand and mud was preserved as the barrier grew over the shoreface (Shawler et al., 2021b).

Trapped sediment from northern Wallops Island provided an easily accessible, ample volume of sand for renourishment of sediment-deprived areas of the beach. And indeed, in 2020–2021 >800,000 m^3 of sand was dredged from the interior of this ~300-m wide beach- and foredune- ridge plain (Alvino et al., 2025). Upon completion of sand extraction, what remained was a shallow (< 2 m deep) tidal pond extending 1500 m alongshore and ~150 m in width, separated from the coastal ocean by a < 100 m wide beach berm and connected to it via a single tidal inlet. Over time, this inlet migrated to the south and rotated, as the backbarrier gradually filled through growth of an expansive (~1000 m^2) sandy flood-tidal delta, along with deposition of finer sands and muds in shallow quiet-water reaches. Successive storms, notably during late summer and early fall 2025, caused overwash and landward migration of the fronting berm, closing in the pond further (Fig. 12). The rapid growth of this flood-tidal delta has led to the infilling of the lagoon, with the majority of the flood-tidal delta now being exposed at low tide. On-site observations made by several contributing authors indicate these exposed sections are quickly being colonized by low-marsh vegetation, including smooth cordgrass (*Spartina alterniflora*), which highlights how inlet processes can support the formation and growth of backbarrier marshes. This process, which typically occurs on decadal to millennial timescales, occurred within only four years along the borrow pit. Ongoing work within the Coastal Geology Lab at VIMS focuses on documenting these processes in real time to better constrain the mechanisms that likely formed the thin, relatively young marshes along the rest of the ESVA.

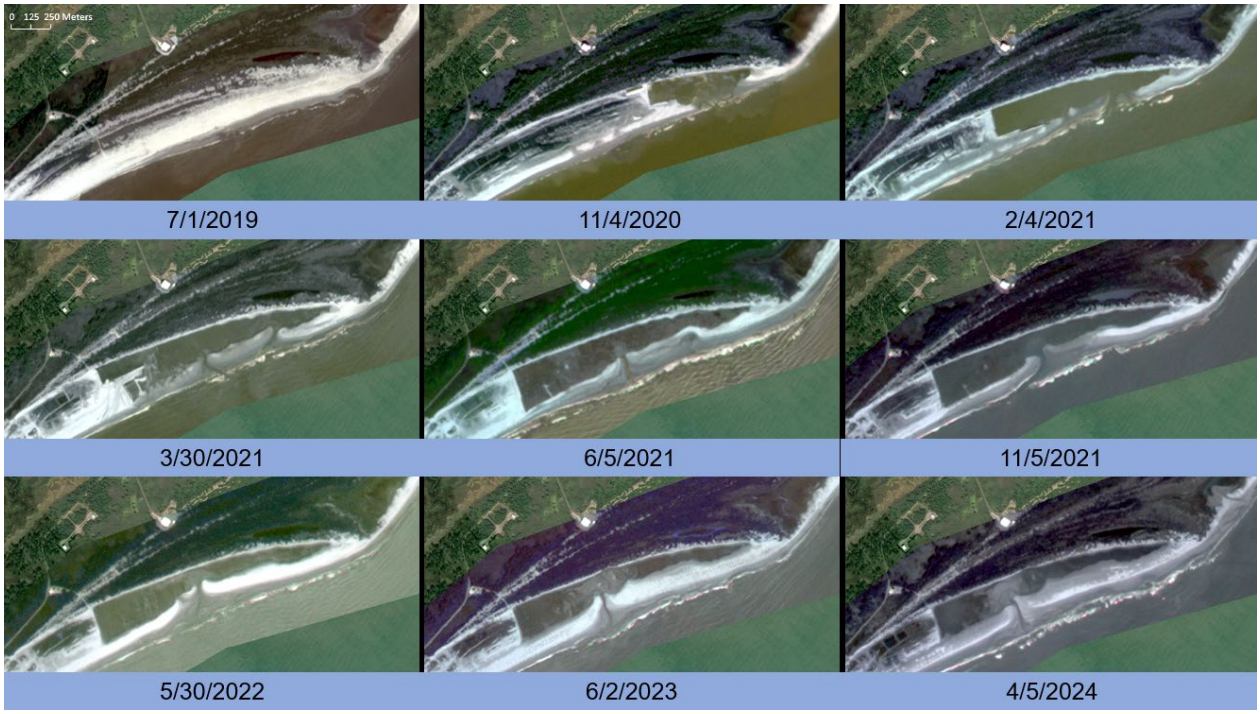

Figure 12. Evolution of the northern Wallops Island beach-and-foredune-ridge sand borrow site over the first four years post-extraction. Since Spring of 2024, the pond has gradually shallowed and narrowed further. As the flood-tidal delta grew, the backbarrier lagoon infilled with fine sediments, and the fronting berm migrated landward. Imagery ©Planet Labs PBC, CC BY-NC-SA 2.0

STOP #4: CHINCOTEAGUE INLET OVERLOOK

After a brief restroom stop at a NASA facility, we'll make our way off Wallops Island, and north back towards CBFS, and then to the east, across southern Chincoteague Bay and onto Chincoteague Island. Our first stop on the island is at its southern tip, Curtis Merritt Harbor, from which we can see Wallops Island. Separating northern Wallops Island from southern Chincoteague and Assateague Islands is Chincoteague Inlet, which you'll see to the south from this overlook. This tidal inlet has an approximately north-south orientation and conveys water and sediment between the Atlantic Ocean and the southern portion of Chincoteague Bay and the northern backbarrier lagoon of Wallops Island (Beudin et al., 2017; McPherran et al., 2021; Georgiou et al., 2023). The inlet is approximately 1.8 km wide, with an 8–12 m deep main ebb channel located on the western margin of the inlet and a shallow (~2 m deep) platform/shoal located to the east of the main channel abutting the Fishing Point spit. The system is microtidal, and the tidal range varies from approximately 1 m near the inlet throat dissipating throughout the backbarrier lagoon to less than 0.15 m in the interior of Chincoteague Bay (Nowacki and Ganju, 2018); its tidal prism is ~44 million m^3 (Jarrett, 1976). During strong wind events, changes in wind direction and intensity drive exchange between Chincoteague Bay and the Atlantic Ocean; during weak wind events, tidal forcing dominates exchange processes (Kang et al., 2017). For example, inflow to Chincoteague Bay through Chincoteague Inlet increases during periods of strong southwest winds, while outflow increases with northwesterly winds (Kang et al., 2017).

STOP #5: FORMATION OF CHINCOTEAGUE ISLAND

Chincoteague Island, today located entirely landward of Assateague Island, was once an open-ocean barrier. The Pocomoke Native Americans originally hunted and fished on the island, which was later occupied by Europeans beginning in the mid-17th century. By the late 19th century, Chincoteague evolved into a fishing village, which today houses a vibrant tourist economy. The island varies in width from approximately 500 to 1500+ m. A series of variably oriented (WSW-ENE and SW-NE) arcuate beach and foredune ridges (< 1–2 m high) are evident on Chincoteague

Island in areas undisturbed by development, particularly in the north (Fig. 13). Immediately to the east, Chincoteague is fronted by Piney Island, which Shawler et al. (2021b) determined is a former part of Chincoteague Island, now separated by a shallow, sand-bottomed tidal channel.

Figure 13. Aerial view of Chincoteague Island looking to the south, with preserved beach and foredune ridges, interrupted by drowned shore-parallel swales, clearly visible. Photo courtesy of G. Campbell, *At Altitude Gallery*, Cape Charles, VA.

This field stop brings us to "Western Ridge", the . . . westernmost . . . ridge on Chincoteague Island. It formed circa (*ca.*) 2250 years ago, part of a landward-migrating barrier island; one which looked markedly similar to Assawoman Island of today. Shawler et al. (2021b) uncovered the geologic history and evolution of Chincoteague Island (along with nearby Assateague Island, which we'll visit later in the day) through stratigraphic (vibracores and Geoprobe direct-push cores), geophysical (ground-penetrating radar [GPR] and seismic), and geochronological data. Their findings are summarized in the evolutionary model shown in Fig. 14. We'll be exploring this model over the course of our next few stops. In short, this is summarized as:

- ***Stage I:*** prior to ~2.25 ka, net landward migration of the barrier system occurred in a regime of slow (~1 mm yr^{-1}) relative sea-level rise.
- ***Stage II:*** around 2.25 ka Wallops Island stabilized offshore of its present location, and the initial progradation of Chincoteague Island was driven by high alongshore and onshore sediment fluxes, primarily via onshore migration of bars. A nodal zone of diverging longshore transport directions developed on Chincoteague, controlled by wave refraction around the southern terminus of Assateague Island (similar to that of today's Wallops Island nodal zone that we explored at the last stop).

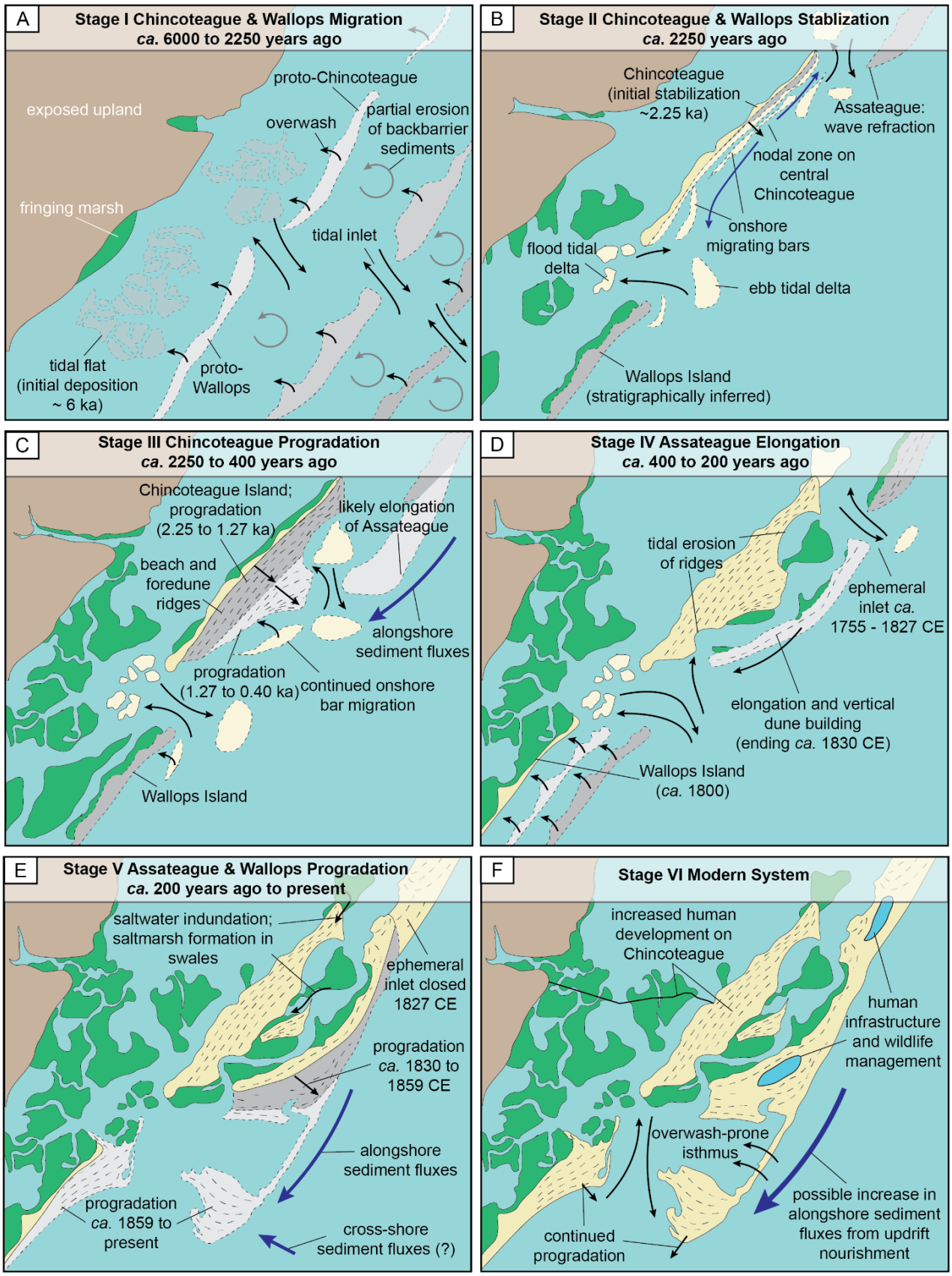

Figure 14. Planform evolutionary model of the Assateague-Chincoteague-Wallops barrier island complex. In all panels, the darkest gray features are oldest, and the lightest gray features are youngest. From Shawler et al. (2021b).

- ***Stage III:*** progradation of Chincoteague continued through progressive welding of bars by inlet sediment bypassing and subsequent reworking of sand by longshore transport processes; the southward elongation of Assateague Island is inferred from the shifting nodal zone evident in the changing ridge orientations on Chincoteague.
- ***Stage IV:*** Assateague Island began to elongate seaward of Chincoteague Island. The exact timing of this development is unknown, but likely between *ca.* 1620 and 1755 CE. The now-closed Cherry Tree Inlet immediately updrift along Assateague, was ephemerally open between 1755 and 1827 CE, resulting in decreased longshore sand fluxes and reduced/halted downdrift progradation. Stabilization of the beach at a single location for this >100 years allowed for gradual growth of the > 8-m tall Lighthouse Ridge (Stop #8) and the growth of fringing marsh atop old barrier sands around the perimeter of Chincoteague Island.
- ***Stage V:*** progradation (net direction NW to SE) of southern Assateague was driven by cross-shore sediment fluxes combined with increased alongshore sand fluxes from closure of updrift inlets, which previously functioned as a sediment trap.
- ***Stage VI:*** the modern system continues to elongate/prograde and is marked by increased human infrastructure such as freshwater ponds for migratory fowl (Assateague Island) and a seawall and offshore breakwaters for erosion control (central Wallops Island).

STOP #6: GROWTH OF THE EXTINCT BARRIER OF CHINCOTEAGUE

At this stop we will attempt to collect some GPR data: be ready to walk the road and check out the data coming in on the small GPR tablet. These data present some of the key evidence supporting the evolutionary history of Chincoteague Island, as presented in Fig. 14b,c. The location of this field stop, as well as that of other data shown in this section of the field trip guide, is given in Figure 15. An example GPR line, collected from this same road, is shown in Figure 16.

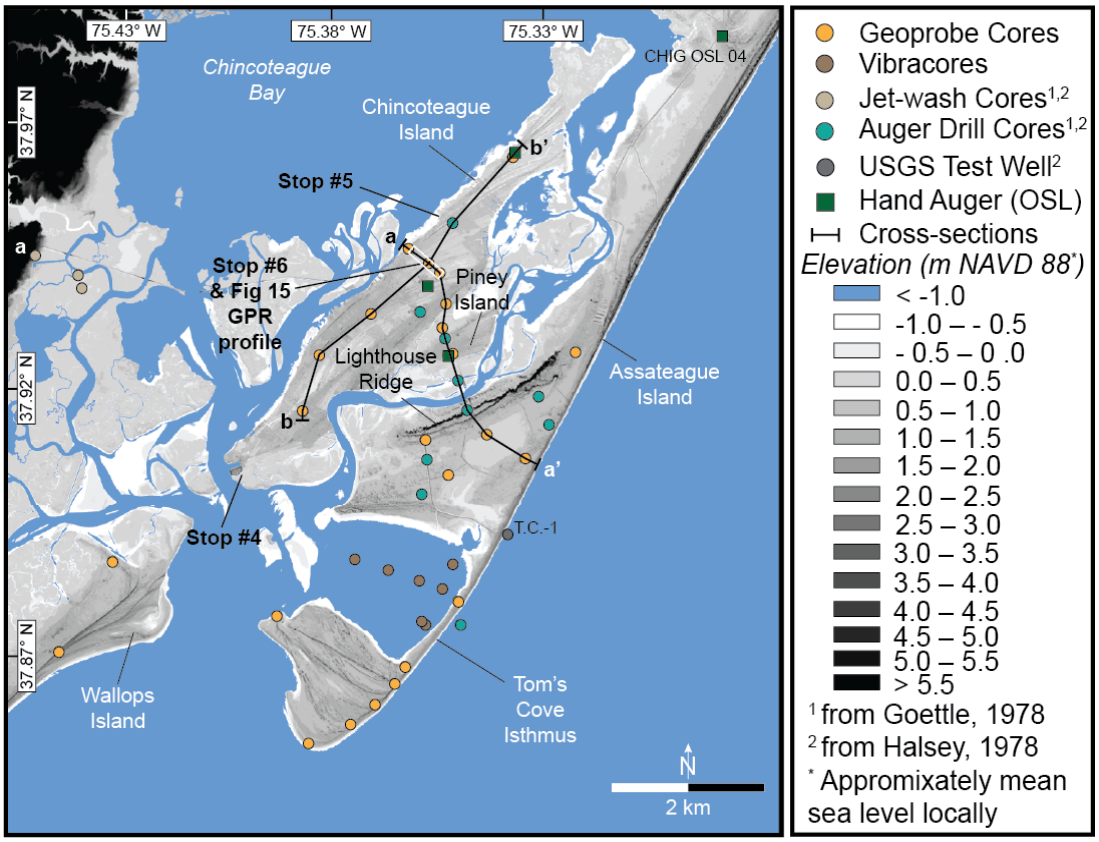

Figure 15. Location of field data shown in Figs. 16 and 17. Digital elevation model is from lidar (USGS, 2016). Figure modified from Shawler et al. (2021b).

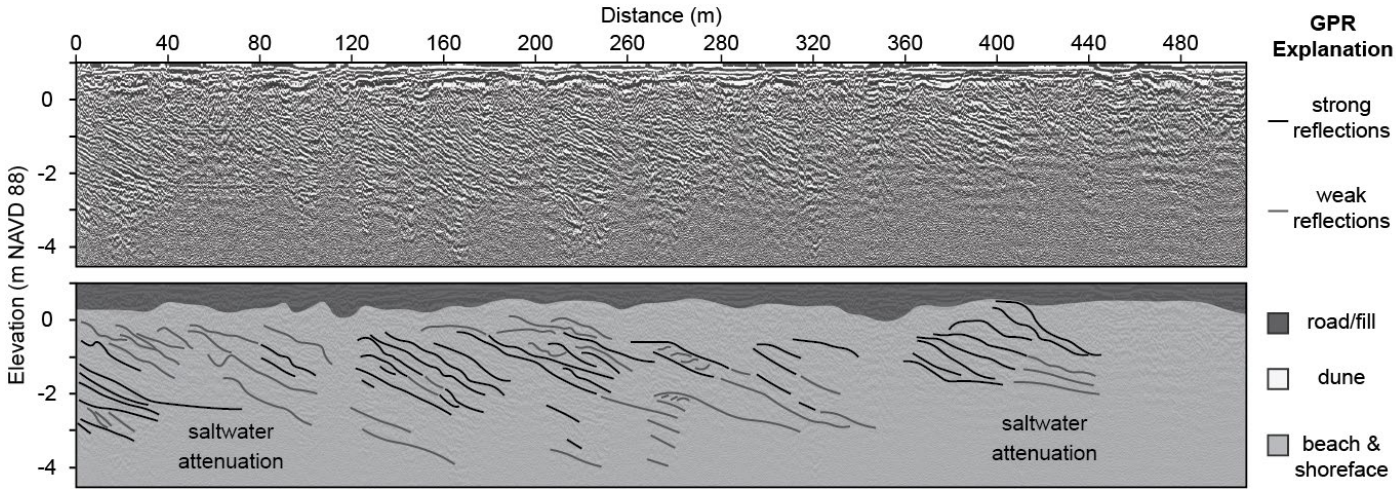

Figure 16. Evidence of seaward progradation revealed by processed (top) and interpreted (bottom) ground-penetrating radar lines from Chincoteague Island. Modified from Shawler et al. (2021b).

Along with new stratigraphic data (Fig. 17) and geochronologic data, GPR data from Shawler et al. (2021b) reveal that initial progradation of Chincoteague Island began ~2250 years ago and lasted until *ca.* 400 years ago. While the net dip directions of reflections in shore-normal radargrams along Chincoteague Island are seaward, there is also evidence of shallow, landward-dipping reflections, indicative of progradation through onshore migration and welding of swash bars. Shawler et al. (2021b) found that progradation of Chincoteague was driven by ebb-delta-associated sediment bypassing at tidal inlets immediately north and south of the island, as observed along inlet-adjacent shorelines throughout the Virginia Barrier Islands. To the north of Chincoteague Island, wave refraction around both an earlier position of Assateague Island's southern end and an ebb-tidal delta associated with the southeast-northwest-oriented inlet separating Chincoteague and Assateague islands likely created a nodal zone on central Chincoteague, much like the one at Wallops at that we visited earlier in the day. Net sediment transport was directed away from this region, both to the north and south along the Chincoteague shoreline. To the north, this sediment entered the semi-protected coastal reach landward of the southern terminus of Assateague Island, and accumulated in a wave-shadow zone in the form of beach and foredune ridges. In this manner, Chincoteague Island underwent a period of widening similar to that observed for modern northern Wallops. The growing shoreface and beach and foredune ridges of Chincoteague Island incorporated approximately 81 x 10^6 m^3 of sand which otherwise would have been transported to downdrift barriers. From *ca.* 2250 to 1300 years ago the barrier volume grew by an average of ~44,000 m^3 yr^{-1} and ~46,000 m^3 yr^{-1} between *ca.* 1300 and 400 years ago (Shawler et al., 2021b).

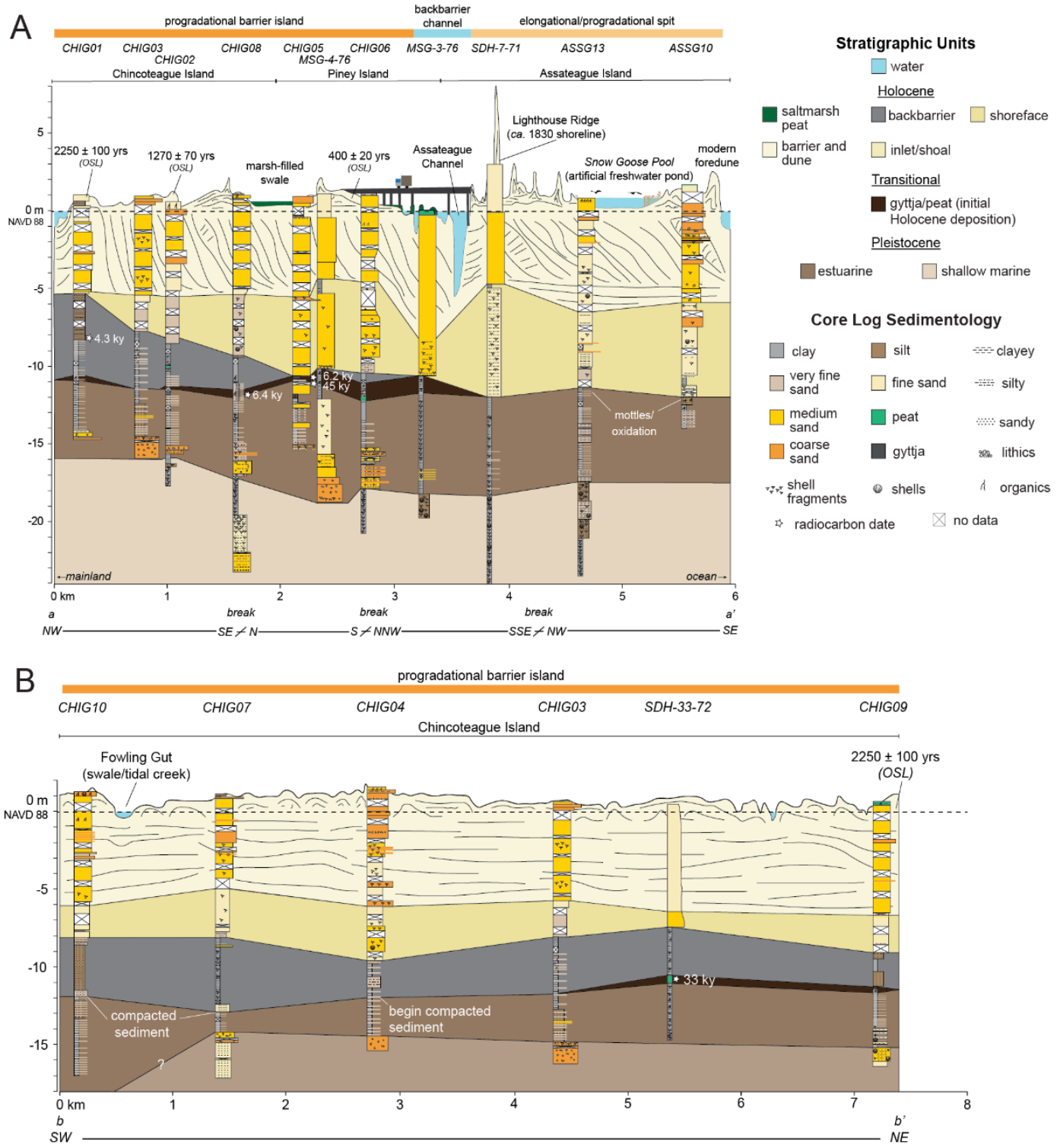

Figure 17. Stratigraphic cross-sections from Chincoteague and vicinity. (a) is oriented approximately west to east on Chincoteague Island and across Piney Island to the relict recurve spit of Assateague. Note multiple changes in orientation given by the "breaks". (b) is oriented southwest to northeast on Chincoteague Island. Internal barrier-island bedding is artistically inferred from GPR profiles. Modified from Shawler et al. (2021b).

STOP #7: LUNCH:

This next stop is where we will have lunch and find a restroom. With much gratitude to Town Manager Mike Tolbert and Town staff, we will have lunch with indoor/outdoor options at The Chincoteague Center (6155 Community Drive, Chincoteague).

STOP #8: ASSATEAGUE ISLAND LIGHTHOUSE

Leaving our lunch spot, we drive over the small tidal channel separating Chincoteague, and its once-conjoined Piney Island. We then cross a larger tidal channel, and jump forward in time, from Piney Island, which formed through barrier progradation ~400 years ago, to Assateague Island, which elongated in front of Chincoteague and Piney islands during the last ~200 years (Shawler et al., 2021b). The best evidence of this history is our next stop: the Assateague Island Lighthouse (Fig. 4). The lighthouse is located on the tallest (height: >8 m) of a series of relict recurved spits which comprise the southern portion of the Assateague Island and are preserved as variably-oriented beach and foredune ridges (generally 1–3 m high). "Lighthouse Ridge" is the location of the *ca.* 1830 CE shoreline, where a coastal navigation light was originally constructed in 1833.

Climbing the lighthouse provides a wonderful view of southern Assateague Island, its spit end "Fishing Point" or "Assateague Hook", the lagoon north of that spit (Tom's Cove), and the narrow (~500 m wide) isthmus protecting Tom's Cove and connecting the hook to the rest of Assateague (Fig. 18). At 58 km in length (from Ocean City Inlet to Fishing Point), the wave-dominated Assateague Island is among the longest islands on the U.S. East Coast. Since around 1830 CE the island has elongated to the south nearly 7 km as a broad plain of beach- and foredune-ridge sets (Fishing Point) grew south from Assateague proper (Fig. 18). This southern spit-end formed in the mid-1800s and was first mapped in 1887 (Shawler et al., 2021b). The isthmus first formed south of the 1859 CE shoreline and by 1910 CE extended over a series of shoals/shoreface ridges. The growth of the isthmus and recurved spit created the shallow Tom's Cove in which fine sediments could settle in the quiet-water embayment over top of the underlying shoreface sediment. The shoals provided comparatively uniform, shallow accommodation which differs from the deeper (>10 m below mean sea level) adjacent shoreface. Recent shoreface mapping (Wikel, 2008) and seismic stratigraphy (Shawler et al., 2021b) indicate the presence of thick (up to 7 m) shoals offshore of modern Assateague that may provide a shallow platform for continued/future spit progradation.

Between the 1800s and 2000, southern Assateague grew at a rate of 21.5 m yr^{-1} and an average short-term (1970 to 2000) rate of 40.3 m yr^{-1} (Hapke et al., 2011) (Fig. 18). In doing so, it experienced a linear increase in island volume of 69×10^6 m^3 (+35%) from 1859 to 2017 (rate: 44×10^4 m^3 yr^{-1}). The main section of Assateague Island (the region north of the 1859 shoreline) gained 12×10^6 m^3 of sand, despite modest landward migration during this time. As it grew, Fishing Point accumulated 43×10^6 m^3 of sand at a long-term (1912–2017) rate of ~40×10^4 m^3 yr^{-1} through southwest elongation via the progressive welding of sand bars and formation of beach and foredune ridges (Shawler et al., 2021b).

A common question—which will make for an excellent point of discussion among our group on the field trip—regards the potential end game for the Assateague hook. What would you predict would be the effect of Assateague Island's continued southerly growth (assuming the same extension rate as today) on the Virginia barrier islands in 100 years? How about 500 years?

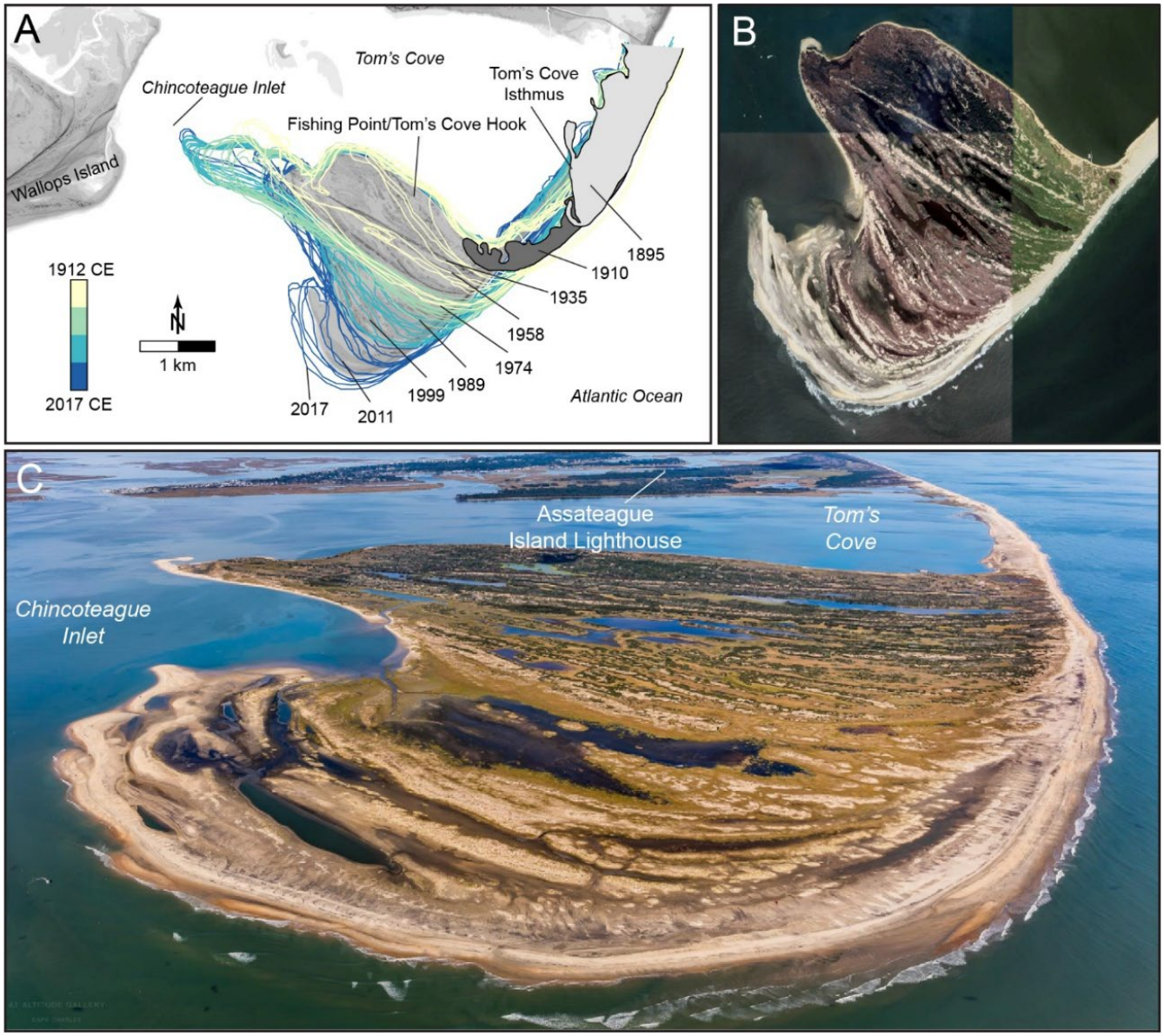

Figure 18. (a) Historical growth of Fishing Point, southern Assateague Island. From Shawler et al. (2021b), as modified from Hein et al. (2019). (b) 2024 satellite image of Fishing Point from Google Earth Pro©. (c) Oblique aerial photo looking north at Fishing Point in *ca.* 2016. The Lighthouse is in the background (your view from the Lighthouse will be southward-facing, the opposite of this). Photo courtesy of G. Campbell, *At Altitude Gallery*, Cape Charles, VA.

STOP #9: CHINCOTEAGUE NATIONAL WILDLIFE REFUGE VISITOR'S CENTER

Today, the U.S. Fish and Wildlife Service manages the southern portion of Assateague Island as a wildlife refuge, though other portions of the island are owned and managed by the National Park Service and Maryland's Assateague State Park. This next stop is another restroom and museum visit, a brief chance to get inside and look around.

STOP #10: ASSATEAGUE ISLAND INTERIOR AND BEACH

The final part of today's tour will include driving some interior trails of Assateague, through the subaerial preserved foredunes and drowned swales that have become exceptional habitat for migratory waterfowl. We'll visit several trails, as time permits; be sure to be on the lookout for continued evidence of the island's progradational history.

Our final stop will allow us to walk around once more, and visit our final beach of the day. This will be at the beach parking lot at the northern end of Tom's Cove Isthmus. An ongoing project seeks to relocate the parking lot and beach access on Assateague Island due to ongoing erosion and landward migration of the isthmus, as well as increasing vulnerability to storm damage. The isthmus has experienced repeated washouts, overwash, and flooding. Repairs, often on the order of $400,000, are required annually to maintain the current beach infrastructure (USFWS, 2024). To ensure long-term, climate-resilient public access and to reduce maintenance costs, officials have decided to move the beach access and parking facilities approximately 4 km north to a more stable location. Once complete, the old beach parking lot will be removed and allowed to return to natural habitat—transforming into dunes, beach, and salt marsh that support wildlife, including threatened shorebirds. Construction is expected to be completed by April 2026.

POST-TRIP: DISCUSSION THOUGHTS, CHINCOTEAGUE TOWN, AND DINNER

That concludes the formal activities during the first day of the field trip. If we haven't done so in the field, some good discussion questions over dinner include:

1. As sea level rises and storm impacts intensify, how should land management agencies prioritize protecting existing infrastructure, retreating from vulnerable areas, or redesigning improvements to coexist with a dynamic coastline? What are the social, economic, and ecological trade-offs of different approaches?
2. How might these decisions differ for residential communities?

Our trip today ends in downtown Chincoteague. Take some time to walk around this classic, quaint beach town. Main Street and downtown are home to quaint shops, galleries, and restaurants. It is great for strolling and souvenir hunting. Further north (though likely closed when we arrive) is the Captain Timothy Hill House, a historic home and one of the oldest structures on the island, which offers insight into 19th-century life on the Eastern Shore.

Dinner will be as a group at Don's Seafood Market & Restaurant (www.donsseafoodrestaurant.com/) right on Main Street in Chincoteague. After that, the bus will bring the group back to the Chincoteague Bay Field Station for the remainder of the evening.

CONFERENCE DAY #3: THE MAINLAND EASTERN SHORE OF VIRGINIA AND SAVAGE NECK SAND DUNES

SUNDAY BACKGROUND

Leaving the seaside barrier islands behind, our final day of the conference brings us down and across the ESVA to the bayside north of Cape Charles, where we will explore a stunning preserve that is home to transgressive Holocene dunes, a robust maritime forest ecosystem, and an eroding bluff beach. Because this site is >1 hour from the CBFS, we've planned a stop along the way at the VIMS Eastern Shore Laboratory (ESL) in the seaside town of Wachapreague, Virginia. Though primarily a stretch and restroom stop, we'll take advantage of the unique setting of Wachapreague to talk about the geology of the mainland Eastern Shore and the barrier islands fronting the central Virginia coast (accessible only by vessel). Field stops are shown in Figure 19.

STOP #11: VIMS EASTERN SHORE LABORATORY, WACHAPREAGUE

Welcome to the Eastern Shore Laboratory, VIMS' outpost in the small (population ~250), low-lying (elevation ~2 m) seaside Town of Wachapreague. The Eastern Shore Lab serves as both a field station in support of research and teaching and as a site for resident research in coastal ecology and aquaculture. Over its 60 plus-year history, the laboratory has become internationally recognized for shellfish research and seagrass restoration, with important contributions to molluscan ecology and aquaculture. It is also the home base for the VIMS Coastal Geology Lab's research across the ESVA and its barrier islands.

Figure 19. Sunday's two field stops.

The Pleistocene Barrier Island of Wachapreague

It may not look it, but ESL is built on the high ground of Wachapreague, site of a former barrier island and dune system. Heading out of town, the land surface dips westward, as one drives across the remnants of the shallow lagoon that once contained salt marshes in the quiet water behind "Wachapreague Island". Farther landward still, the terrain begins to gradually rise towards the central spine of the Eastern Shore along Rt. 13. Here, the landscape is characterized by ridge and swale topography (Fig. 20), nearly identical to that which we observed on Chincoteague and Assateague islands, and once again providing evidence of coastal progradation.

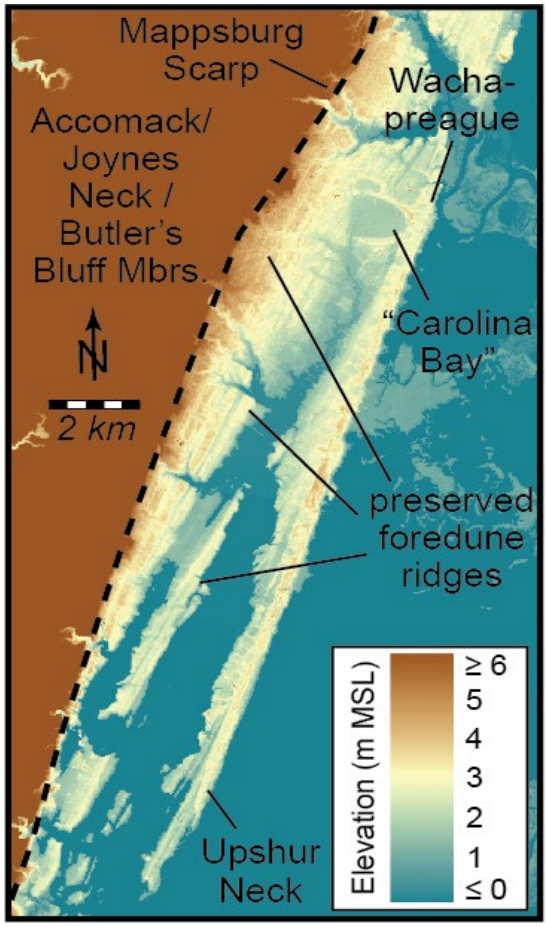

Figure 20. Lidar-derived topographic-bathymetric map of the Wachapreague Formation (Fm.), showing the morphology of preserved foredune ridges, particularly within the western Locustville Member (Mbr).

Together, these features—the Wachapreague barrier and backbarrier and the progradational beach ridge and foredune plain landward of it—form the Wachapreague Formation (Fm), which Cahoon et al. (2025) recently revealed is comprised of two unique members. The western Locustville Member (Mbr) (type section: Fig. 21) is 10–20 m thick and comprised of three conformable facies: (1) lowermost beds composed of dark gray shelly clayey silt that sometimes includes interbedded layers of muddy coarse sand; shells include disarticulated or intact dwarf clams (*Mulinia spp.* and *Spisula spp.*) and periwinkle snails (*Littoraria irrorata*); (2) grayish-brown well-sorted, well-rounded, micaceous, quartz-rich, very fine to fine sand in which mica and heavy minerals account for up to 20% of the sedimentary matrix; and (3) firmly compacted, pale-brown medium sand with heavy mineral lamellae and few laminations of granules and pebbles. The Locustville Mbr. lies at an elevation of +3.5 to -1.0 m above modern mean sea level (m MSL) and decreases in elevation from west to east. To the east, and containing the remnants of Wachapreague Island, is the Upshur Neck Mbr. (type section: Fig. 22). This unit is 5.0–8.0 m thick and comprised of upward-coarsening sand. Lower beds in this unit consist of brown or gray well-sorted, well-rounded, fine sandy silt and silty fine sand. Following an abrupt contact, these beds are overlain by brown or dark yellowish-brown poorly sorted, subangular, silty, medium-coarse sand with interbedded layers of pebbles and granules throughout. The Upshur Neck Mbr. lies at an elevation of 0.0 to -1.0 m MSL and is characterized by sequential, southward-oriented recurved ridges. Type sections for each of these two new members, as developed by Cahoon et al. (2025) are provided in Figures 21 and 22.

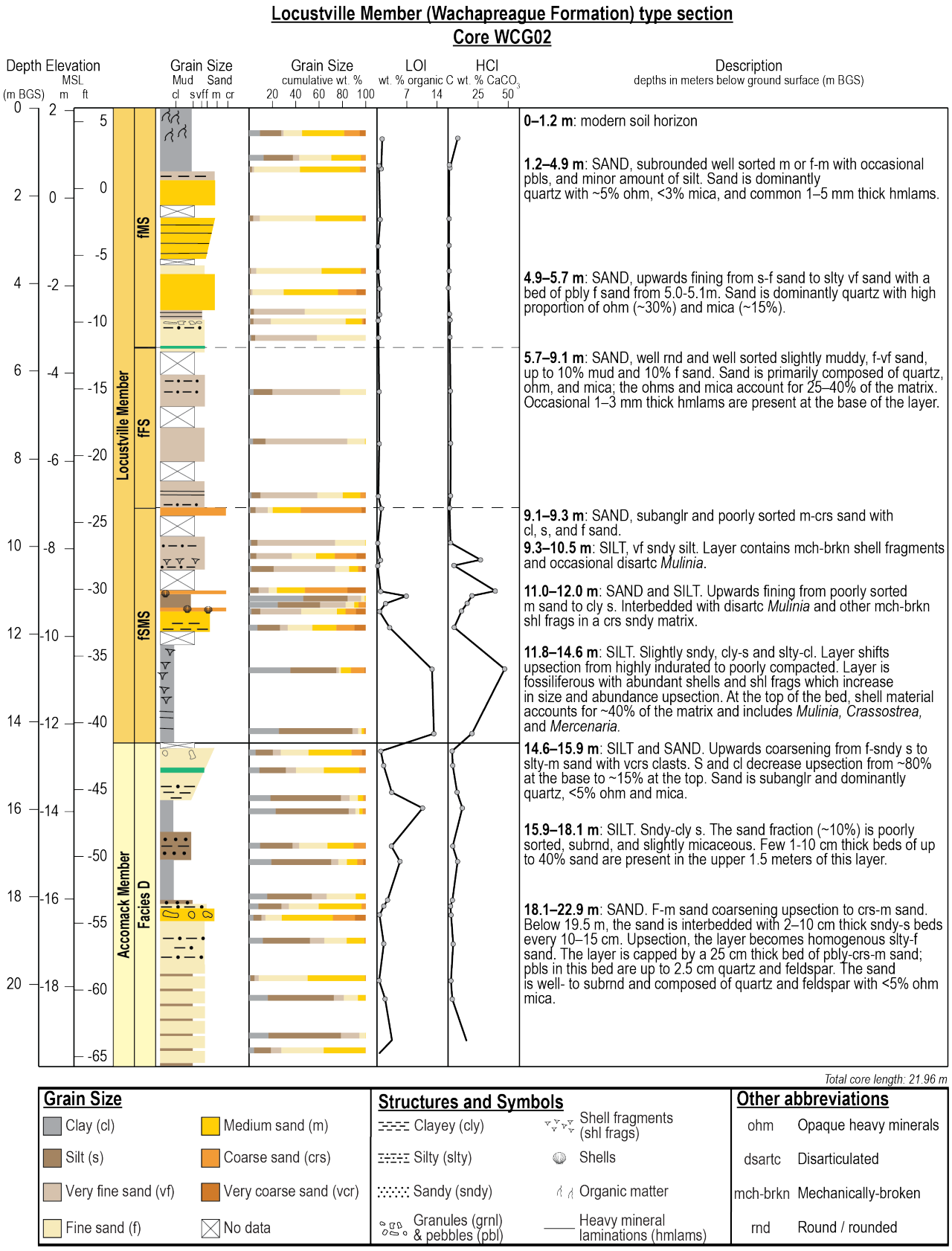

Figure 21. Locustville Member type section, from core WCG04 of Cahoon et al. (2025).

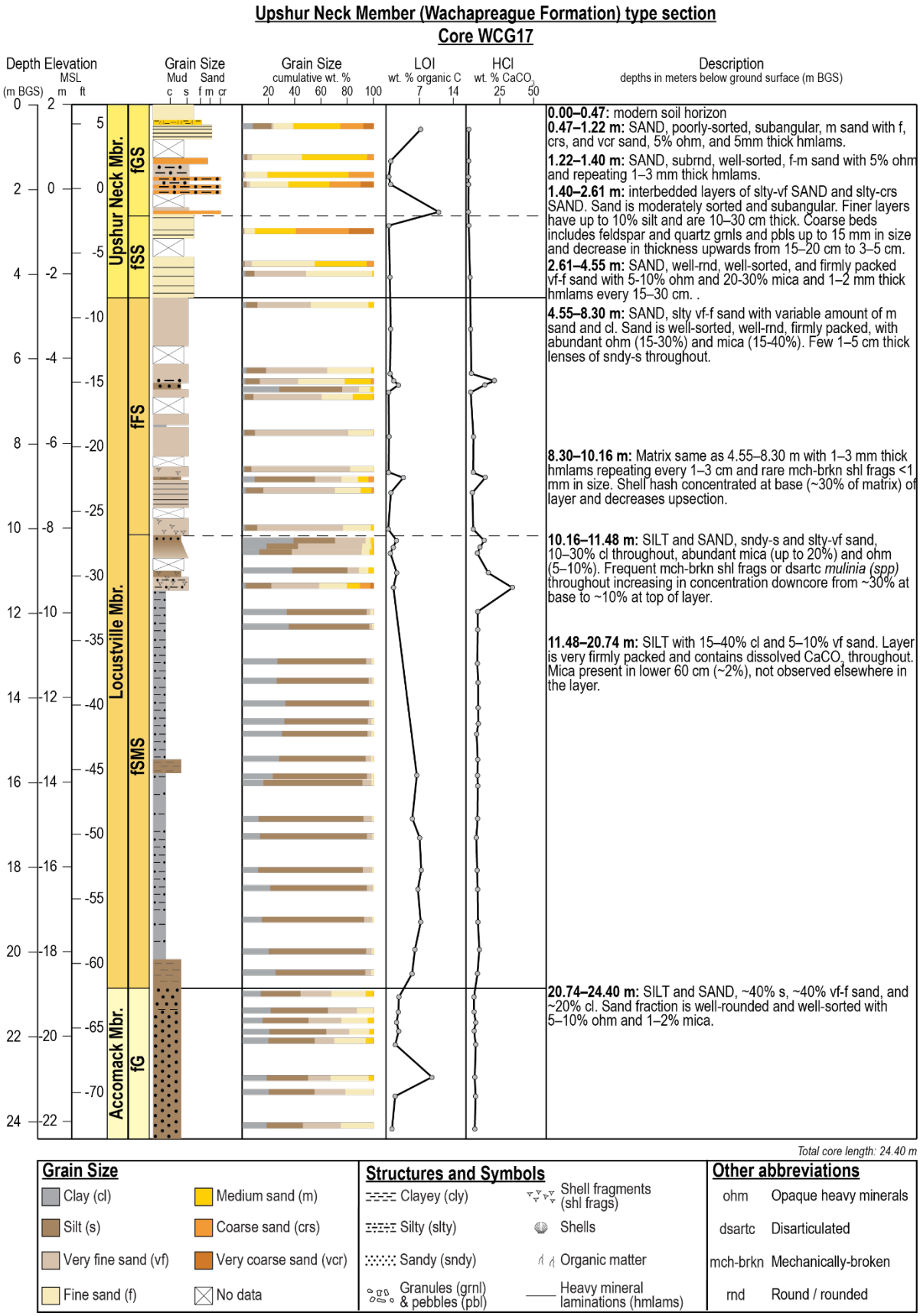

Figure 22. Upshur Neck Member type section, from core WCG17 of Cahoon et al. (2025).

Cahoon et al. (2025, 2026) identified the Locustville and Upshur Neck Mbrs as a progradational beach- and foredune-ridge plain and transgressive barrier/spit system, respectively. Much like the Holocene barrier island of Chincoteague, stratigraphic sections (Fig. 23) and GPR records (Fig. 24) reveal clear evidence of transgression and highstand (in the form of preserved barrier island facies along the landward margins) followed by beach and shoreface progradation. Both units are partially obscured by a thin (< 2 m) aeolian sand likely formed during the MIS 2 (Fig. 2) glaciation and lowstand. This sheet was partially shaped into hundreds of elliptical depressions called "Carolina Bays", which range in size from 250–300 m to upwards of 2 km in diameter, and most likely originate from post-depositional reworking by congeliturbation (Lundine and Trembanis, 2025). More recent work by Cahoon et al. (2026) advanced understanding of the history of the Wachapreague Fm. and adjacent depositional units, in part through new geochronology. They found that Pleistocene deposits on the ESVA record evidence of five marine transgressions and highstands during which water levels reached elevations near or higher than today, during MIS 5 and MIS 3 (Fig. 2), a sequence of events summarized in Figure 25.

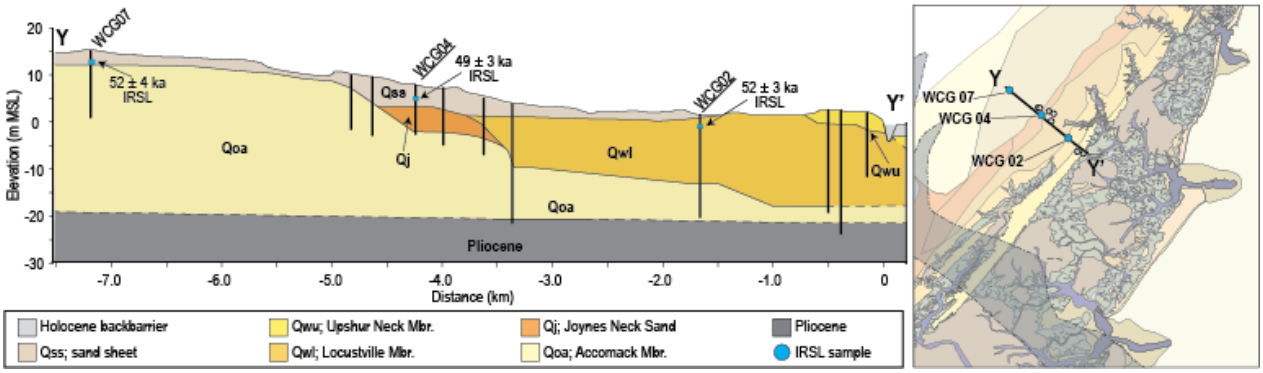

Figure 23. Stratigraphic section taken across the Pleistocene (MIS 7 to present) units composing the seaside Eastern Shore of Virginia. The eastern end of the profile (Y') runs through downtown Wachapreague, only several hundred meters from the ESL field stop. Note that the Upshur Neck Mbr. barrier sits unconformably atop the Locustville Mbr, and forms the "high" ridge upon which Wachapreague sits. Figure from Cahoon et al. (2025)

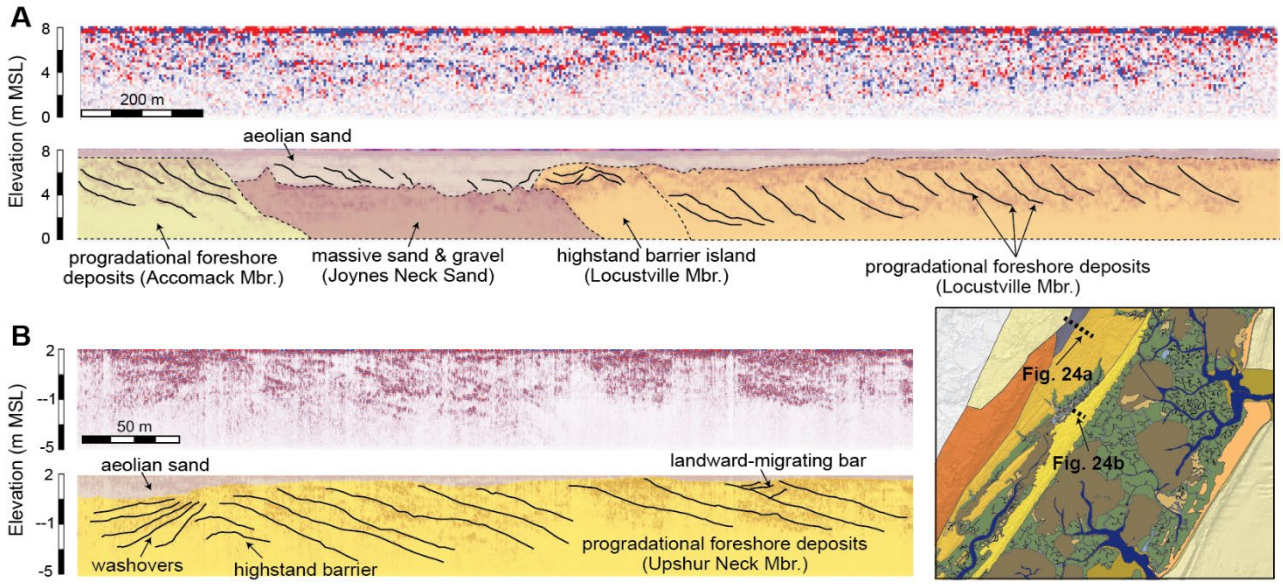

Figure 24. Examples of ground-penetrating radar (GPR) radargrams capturing Pleistocene coastal deposits along the Eastern Shore seaside near Wachapreague, Virginia. Records capture (a) the highstand barrier, dune, and progradational beach-ridges of the western margin of the Locustville Member (Mbr) of the Wachapreague Formation (Fm); and (b) transgressive washover and progradational foreshore deposits of the Upshur Neck Mbr of the Wachapreague Fm. GPR profile locations are shown in inset in bottom right. Derived from data presented by Cahoon et al. (2025, 2026).

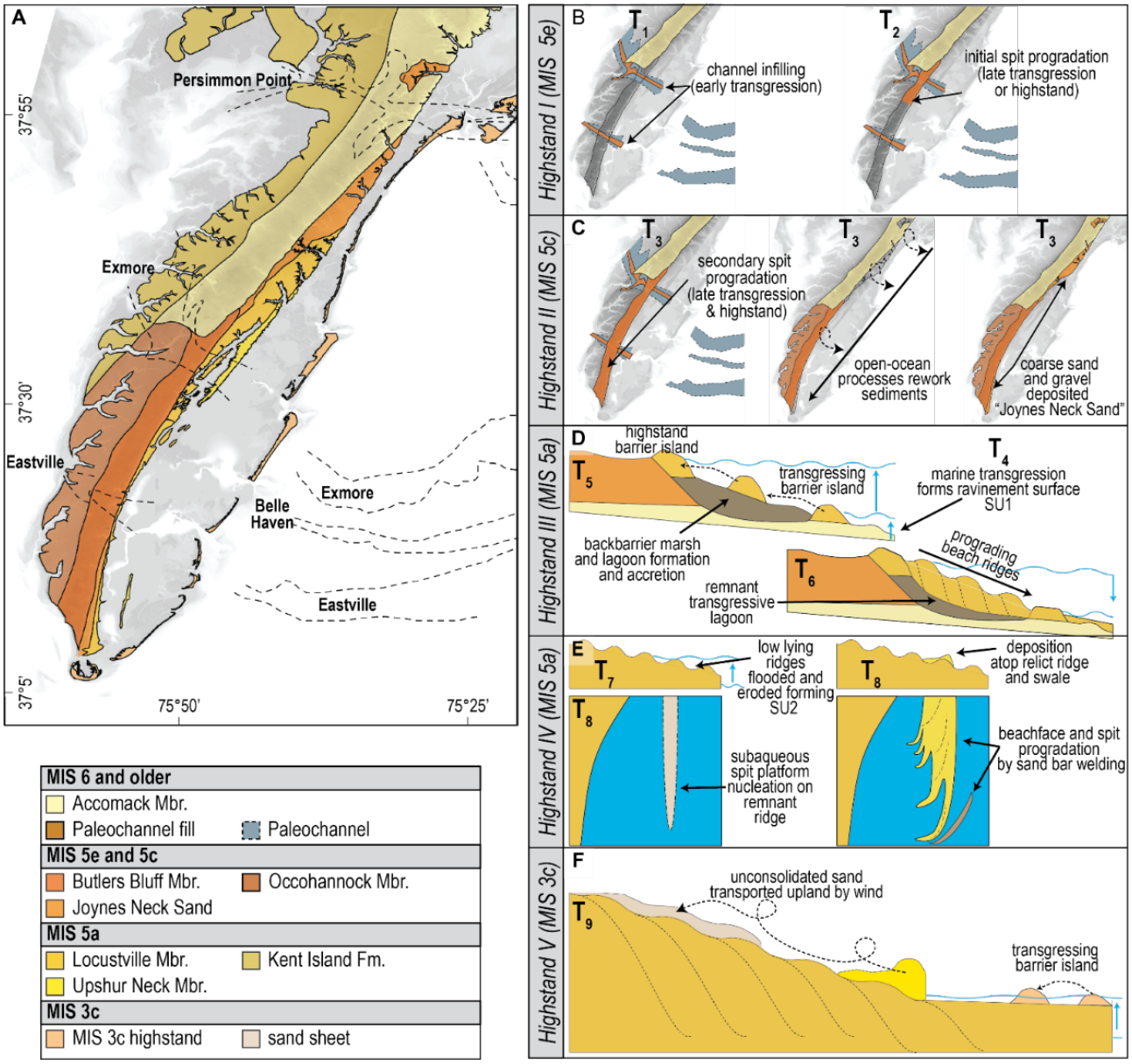

Figure 25. Updated depositional model for the Late-Pleistocene geologic units found on the Eastern Shore of Virginia. "T_x" indicate relative times with unique depositional systems determined by stratigraphic position and geochronology. Digital elevation model in (A) and (B) from Faunce and Rapp (2020). Paleochannel map in (A) reconstructed from McFarland and Beach (2019) and Brothers et al. (2020). Figure modified from Cahoon et al. (2026).

The Modern Barrier Islands Offshore of Wachapreague

Next, we turn our attention back towards the Atlantic Ocean one final time. Standing at the ESL boat basin, you'll see in the distance (~8 km) a line of coastal pines. This is Parramore Island, a > 1-km wide barrier characterized by a series of preserved progradational dune ridges and swales, including the nearly 9-m tall, ~250-year-old "Italian Ridge". Raff et al. (2018) described the complex history of this island: following a period of rapid overwash-driven retrogradation, and coinciding with a period of slow relative sea-level rise (~1 mm yr^{-1}), Parramore stabilized ~1000 years ago in partial response to pinning by and sediment delivery from erosion of a Pleistocene-aged antecedent high (which Cahoon et al. [2026] identify as a MIS 3 highstand barrier ridge buried at only -6 m MSL).Following pinning, Parramore built seaward through development of successive progradational beach and dune ridges. These processes were interrupted by inlet formation—possibly associated with an interval of enhanced storminess—at least three

times during this period. Following inlet closure in the early 1800s, island progradation was rapid, with Parramore Island reaching its maximum width *ca.* 150 years ago. Since then, Parramore has experienced severe erosion while remaining in place: it has lost 68×10^6 m^3 (−56%) of its mid-1800s volume at a near-linear rate of 460,000 m^3 yr^{-1} (Fig. 26a).

In stark contrast to Parramore is its neighbor to the north, Cedar Island, which you cannot see from the mainland. Cedar is low (active sand dunes < 2 m tall) and narrow (~150 m). This striking difference from Parramore is due to Cedar's geologic history: stratigraphic and geochronologic evidence indicate that Cedar Island was once progradational, wider than present by at least 1 km, and likely characterized in at least its center by several beach and foredune ridges oriented sub-parallel to the modern beach (Shawler et al., 2019). Although the exact island and ridge dimensions are not preserved, the morphology of Cedar Island likely resembled that of the mid-1800s Cobb Island or modern Parramore or Hog islands, as opposed to its present low, overwash-dominated state. By the early 1800s Cedar Island had become largely erosional (Shawler et al., 2019), and it has since maintained a similar (narrow) width through time, migrating landward and nearly parallel to the mainland Delmarva shoreline (Robbins et al., 2022; Fig. 26b).

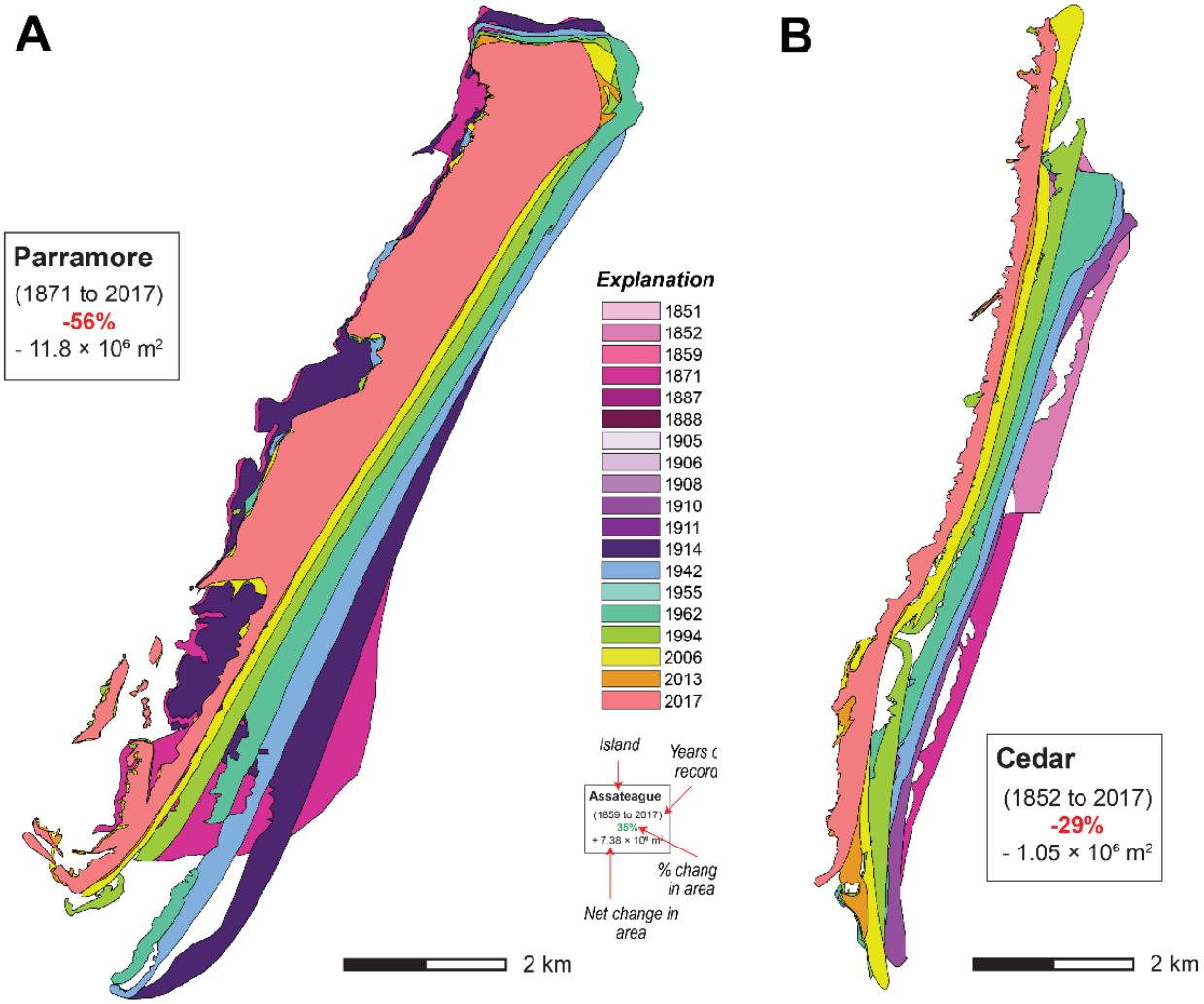

Figure 26. Area and relative position of (a) Parramore Island and (b) Cedar Island from the mid-1800s to 2017 CE. Consecutive outlines of each island are overlain at the same scale and in georeferenced relative positions. Modified from Robbins et al. (2022).

The dichotomy between these two adjacent islands—the wide, tall Parramore which is today eroding but last experienced overwash > 1000 years ago, versus the low, narrow, and actively migrating Cedar—has made them ripe for study of mesoscale barrier island behavior over periods of decades to centuries. Detailed exploration of the geologic history of each (Finkelstein and Ferland, 1987; Raff et al., 2018; Shawler et al., 2019) has allowed for exploration of causal mechanisms responsible for these differing behaviors, including antecedent topography (Shawler et al., 2021a), autogenic inter-island sand exchanges (Robbins et al., 2022), and lags in barrier response to sea-level rise caused by slow removal of an island's "geomorphic capital" (Mariotti and Hein, 2022). It also allows for, in the future, investigation of the development of different ecological systems associated with divergent physical dynamics within the same overall coastal environment.

As fodder for discussion, some questions under consideration by geologists studying these islands include:

1. What factors may control Parramore Island's future fate in 100 years?
2. Will it become geomorphologically similar to Cedar Island?
3. How far south might this trend continue?
4. What is the fate of the "rotational" Virginia Barrier Islands into the geologic future?

STOP #12: SAVAGE NECK SAND DUNES AND BEACH

Our final stop—after another 40-minute drive from Wachapreague—is the Savage Neck Sand Dunes Natural Area Preserve. Parking there is limited, so we'll ask that everyone first stop at the Northampton County Administrative Building (16404 Courthouse Road, Eastville) and gather into as few vehicles as possible for the final ~10 minutes of the drive.

The 298-acre Savage Neck Sand Dunes Natural Area Preserve is protected and managed by the VA Department of Conservation and Recreation (Wilson and Tuberville, 2003). It contains a Chesapeake Bay beach, dunes, a freshwater pond, maritime forest communities, migratory songbird habitat, and the largest population of the federally protected northeastern beach tiger beetles (*Habroscelimorpha dorsalis dorsalis*). Bare areas within dunes host populations of the globally rare sea-beach amaranth (*Amaranthus pumilus*). We'll take a ~20-minute walk along meandering paths through the dunes, and make our way out to the beach. Unfortunately, high tide is predicted for 1:25 pm on Sunday, so water levels will be rising quickly as we arrive: some of the features along the beach described below may not be visible.

A Massive Late Holocene Dune Field

Built atop the Occohannock and Butler's Bluff Mbrs of the Nassawadox Fm, the Savage Neck Sand Dunes extend 2.9 km along the bayside shoreline of the southern ESVA, largely as a long, narrow (~200 m) laterally continuous ridge with few breaks. Dunes can reach elevations of > 17 m MSL, with slopes within the dune field of >50º (Fig. 27; Davis, 2020).

Scarping of the dune along the Savage Neck Beach reveals a 5-m tall outcrop in which two units were identified and described by Davis (2020; Fig. 28). The lower unit is a clay-rich paleosol subdivided into upper and lower sub-units that differ in terms of soil texture and color, and are indicative of 2Ab (massive, dark grayish brown loamy sand), 2Beb (massive light olive brown clay loam), and 3ABt (massive, yellowish-brown sandy loam) horizons. Situated above this paleosol is a sharp contact with the upper unit, a very pale brown medium-grained, subrounded, moderately well sorted, quartz-rich sand with abundant root traces, and shallow planar and cross beds near the surface. Further, Davis (2020) finds that these units are laterally continuous along the southern bayside ESVA shoreline to Latimer's Bluff, near the mouth of the Chesapeake Bay. Two archeological sites containing Middle to Late Woodland period artifacts have been recorded within the paleosol (Lowery, 2016). Radiocarbon dating provides a maximum age of 1100 CE for the initiation of the dune field (Cline, 2001; Lowery, 2016; Rick et al., 2015; Davis, 2020). Additional dating by Davis (2020) suggests that active deposition/ migration of the dune

field continued as late as the 1700s CE, when they transgressed over the peat at Butler's Bluff and engulfed trees at Savage Neck.

Evidence for the mechanisms responsible for late Holocene dune formation, transgression atop the Pleistocene substrate, and eventual stabilization is inconclusive. Davis (2020) posits three hypotheses for the mechanisms underpinning the erosion of sands of older Pleistocene units (including the aeolian sand sheet of Cahoon et al. [2025]) and reworking by wind to form the Savage Neck Dunes: (1) landscape denudation due to widespread anthropogenic burning; (2) protracted drought during the 900–1300 CE Medieval Warm Period, which was characterized by warm, dry conditions in North America, including the Chesapeake Bay region (Stahle and Cleaveland, 1994; Cronin et al., 2000, 2003; Willard et al., 2003); and (3) late Holocene tidal amplification which may have allowed for extended daily periods of drying of a newly expanded intertidal zone, allowing for aeolian erosion and reworking. To date, none of these hypotheses have been tested.

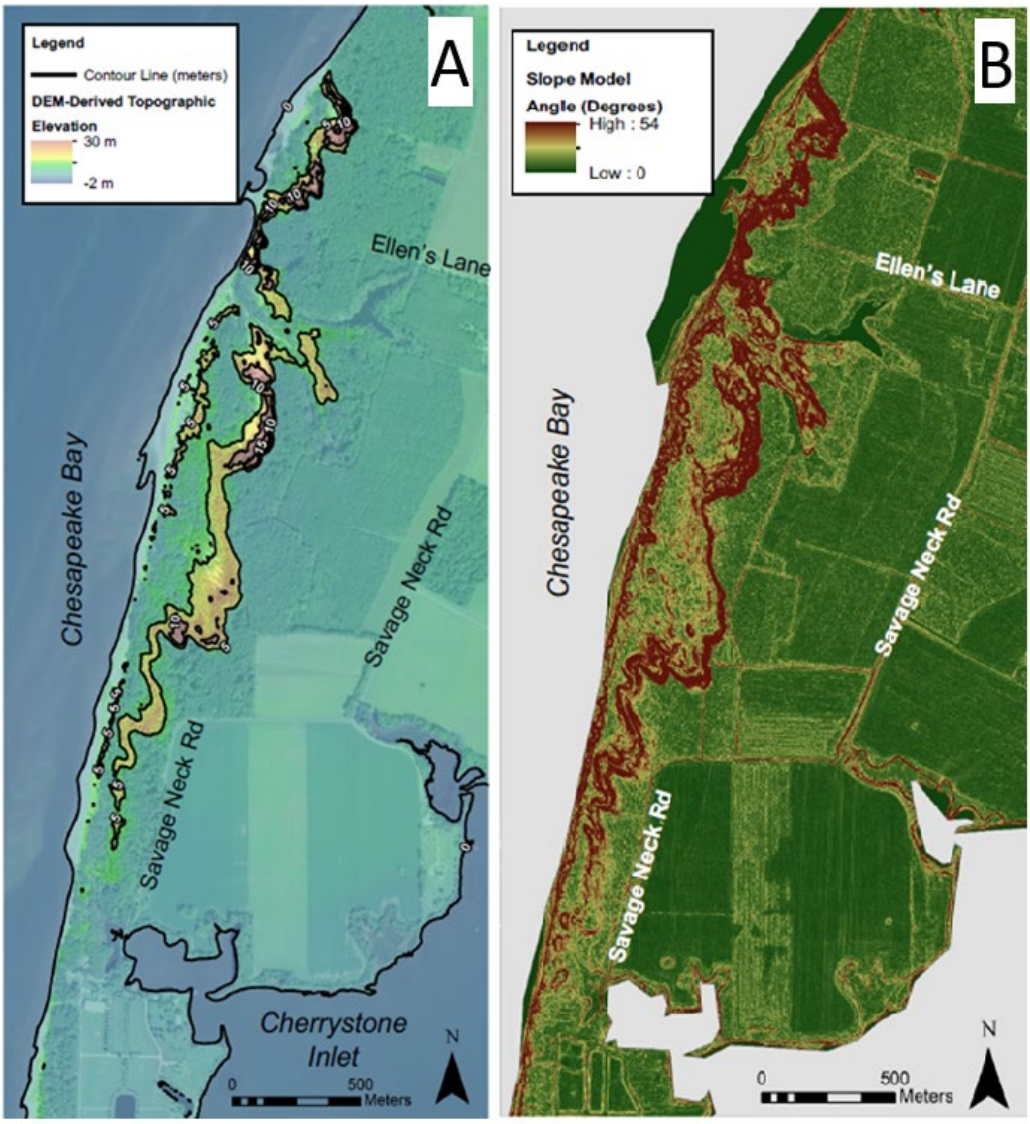

Figure 27. Digital elevation model (a) and slope model (b) of the Savage Neck Sand Dunes. Elevation data are from USGS and NOAA (OCM Partners, 2019), and associated contour interval is 5 m. Figures from Davis (2020).

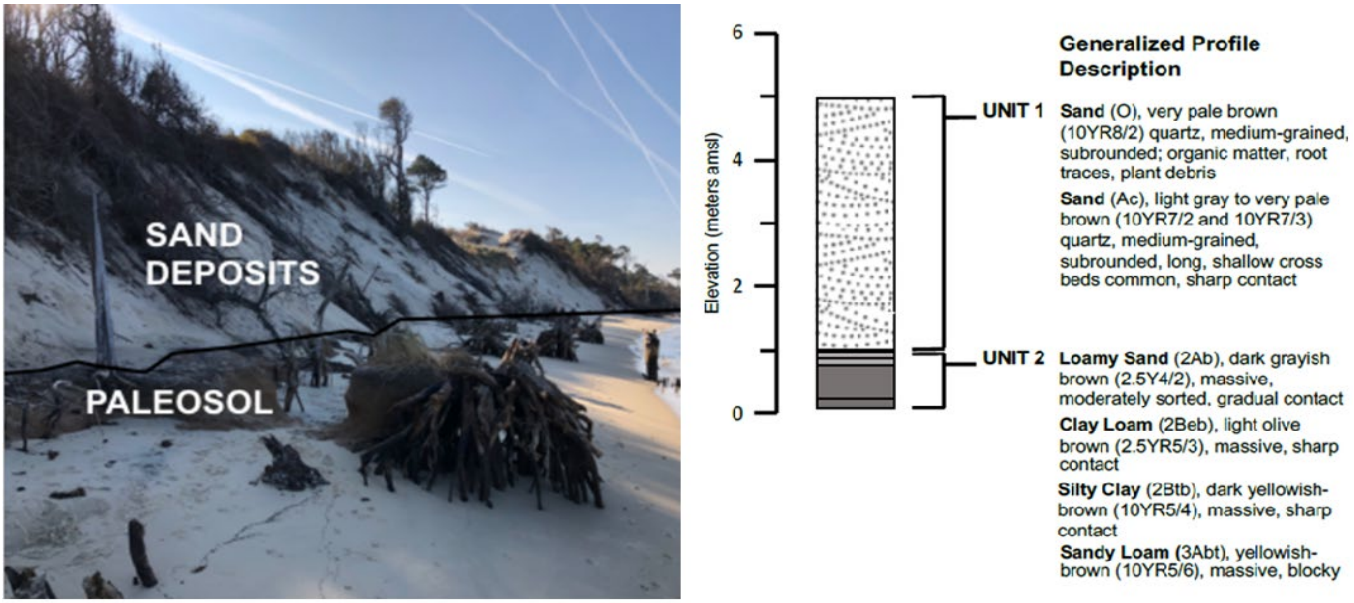

Figure 28. Stratigraphic profile of the "outcrop" (erosional scarp) of the Savage Neck Dunes from the adjacent beach. Figures from Davis (2020).

Disappearing Dunes: Erosion of the Savage Neck Bluff

We will step out onto the (likely very narrow) beach at Savage Neck for a final, quick view of coastal processes. Unlike the open-ocean barrier islands of the seaside, the dominant coastal process along the Chesapeake Bay shoreline is erosion—and there is plenty of evidence for it right in front of us at Savage Neck Beach.

At the northern portion of Figure 27a, the high-elevation dunes intersect the shoreline (west of Ellen's Lane). This is the northern limit of the natural area preserve where it transitions to private property. Long-shore sediment transport is from north to south, carrying high flux of sediment. Because of the shape of the shoreline, it has been eroding, and the private property owners constructed a set of three rubble mound breakwaters in 2008/2009 (note the size difference of these compared to those at Wallops Island). Due to the southerly longshore sediment transport, these breakwaters were designed to be attached to the shoreline with tombolos. These were constructed with sand brought from offsite in an attempt to mitigate the impact on the downdrift shoreline from the sand being trapped by the breakwaters. In addition, sand was placed south of the southern breakwater to provide a source to the natural area preserve (Fig. 29).

Aerial photos and ground observations made after breakwater and sand emplacement illustrate the effect of these engineering interventions on the coast. Starting within a year after construction, the northern breakwater began to fill with sand transported from updrift (north) by the strong littoral current, while the sand source south of the breakwaters was transported downdrift (south) along the natural area preserve (compare Figs. 29 and 30). The tombolo behind the southern breakwater also began to shift northward as the beach south of the breakwater was reworked by waves refracting around the end structure to form a spiral beach. By 2020, the beach at the southernmost breakwater had eroded sufficiently far into the dune that an existing house was relocated to the northeast in 2021 (Fig. 30).

Recently, there has been an increase in construction of both houses and additional breakwaters along the reach north of the natural area preserve. Based on the previous observations, as more breakwaters are constructed north of the initial set of three, they may accumulate additional sand from long-shore sediment transport. Currently, the beach south of the structures is very narrow and characterized by fallen trees and the high, eroded scarp of the Holocene dunes (Fig. 31).

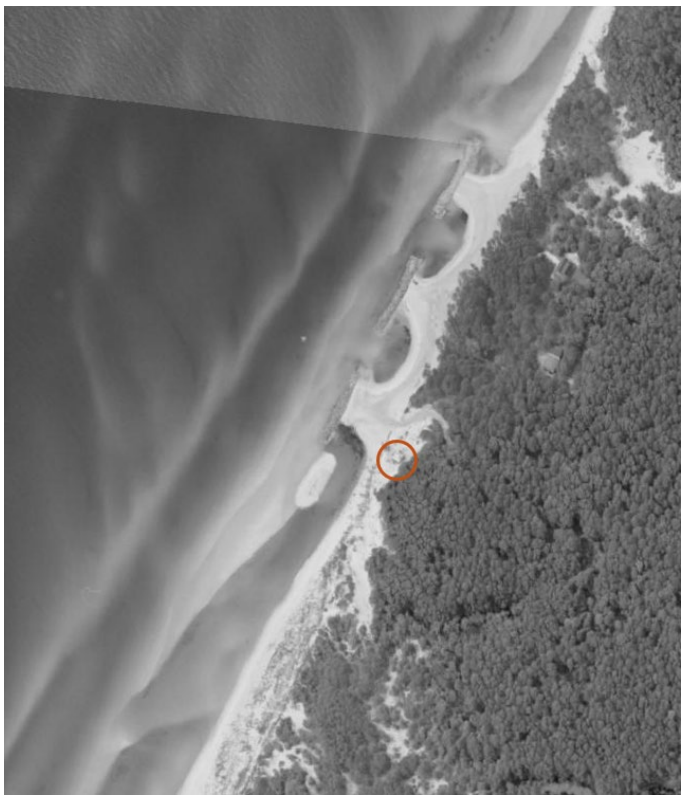

Figure 29: Aerial image of the three breakwaters and offshore sand source in summer 2009, shortly after construction. The red circle indicates the white house seen in subsequent figures; north is up (imagery courtesy of the VIMS SAV Monitoring Program).

Figure 30: Aerial images (north is up) of the breakwaters from summer 2020 (left) and 2021 (right). The red arrow in the 2021 image shows the movement of the small house away from the scarped bank. Also note the volume of sand trapped behind the breakwaters as compared with that in figure 29 (imagery courtesy of the VIMS SAV Monitoring Program).

Figure 31: Oblique aerial image from 6 February 2026 looking northeast at the southernmost breakwater and the northern portion of the Savage Neck Natural Area Preserve shoreline. Landward of the small white house (noted in figures 29 and 30), a clearing can be seen on top of the Holocene dunes where a house is being built. South of the private property (to the right in the image) the steep scarped banks can be seen with dead trees at its base. (Image courtesy Emily Hein, VIMS)

CLOSING

Leaving the beach and dunes at Savage Neck, participants will return to their vehicles, head back to the Northampton County Administrative Building (16404 Courthouse Road, Eastville) to pick up any remaining vehicles, and start the drive home. For most this will take them south over the Chesapeake Bay Bridge Tunnel. Before that is a turnoff to Cape Charles (Google it!), which has a number of excellent shops and restaurants. For a quicker lunch stop, a large Royal Farms is on the right (southbound) side of Rt. 12 and makes for an excellent stop before crossing the bay. About 20 minutes later (seriously: take your time, local authorities will ticket along this stretch), you'll reach Virginia Beach, where the options are endless. Safe driving!

REFERENCES

Alvino, C., Lapenta, K., Sweeney, C., Call, M., Lipford, A., Gehman, L., Staengl, E., Karpanty, K., 2025. *Ecological Impact Assessment and Mitigation Plan for Shoreline Stabilization at NASA's Wallops Island Flight Facility: Annual Report for the 1 April 2024–31 March 2025 Reporting Time Period*, Contract DWR-403-2024-0029, 66 p.

Barksdale, M.B., Hein, C.J., Kirwan, M.L., 2023. Shoreface erosion counters blue carbon accumulation in transgressive barrier-island systems. *Nature Communications*, v. 14, p. 8425. https://doi.org/10.1038/s41467-023-42942-8.

Barnes, B.M., Truitt, B.R. eds., 1997. *Seashore Chronicles: Three Centuries of the Virginia Barrier Islands*. University of Virginia Press. 282 p. https://www.upress.virginia.edu/title/2466/.

Bemelmans, C.B., Stalk, C.A., Ciarletta, D.J., Miselis, J.L., 2025. *Coastal multibeam bathymetry and backscatter data collected in June 2024 from Wallops and Assawoman Islands, Virginia*: U.S. Geological Survey data release, https://doi.org/10.5066/P14SGUMT.

Beudin, A., Ganju, N.K., Defne, Z., Aretxabaleta, A.L., 2017. Physical response of a back-barrier estuary to a post-tropical cyclone. *Journal of Geophysical Research: Oceans*, v. 122, p. 5888–5904. https://doi.org/10.1002/2016JC012344.

Boon, J.D., Mitchell, M., 2015. Nonlinear change in sea level observed at North American tide stations. *Journal of Coastal Research*, v. 31, p. 1295–1305. https://doi.org/10.2112/JCOASTRES-D-15-00041.1.

Brothers, L.L., Foster, D.S., Pendelton, E.A., Baldwin, W.E., 2020. Seismic stratigraphic framework of the continental shelf offshore Delmarva, U.S.A.: Implications for Mid-Atlantic Bight evolution since the Pliocene. *Marine Geology*, v. 428, p. 106287. https://doi.org/10.1016/j.margeo.2020.106287.

Cahoon, K.M., Hein, C.J., Fenster, M., Clarke, C., Ramsey, K.W., 2025. Updated stratigraphic mapping reveals insights into the late Pleistocene evolutionary history of the Virginia Eastern Shore, US Mid-Atlantic Coast. *Stratigraphy*, v. 22, p. 99–134. https://doi.org/10.29041/strat.22.2.02.

Cahoon, K.M., Hein, C.J., Fenster, M.S., Huot, S., 2026. Refined Late-Pleistocene Evolutionary and Sea-Level History for the Delmarva Peninsula, US Mid-Atlantic Coast. *Marine Geology.*

Cline, J.W., Monaghan, G.W., Hayes, D.R., 2001. *Archaeological and Geological Evaluation at Butler's Bluff, Northampton County, Virginia*. William & Mary Center for Archaeological Research, Williamsburg, VA.

Colman, S.M., Halka, J.P., Hobbs III, C.H., Mixon, R.B., Foster, D.S., 1990. Ancient channels of the Susquehanna River beneath Chesapeake Bay and the Delmarva Peninsula. *Geological Society of America Bulletin*. V. 102, p. 1268–1279. https://doi.org/10.1130/0016-7606(1990)102<1268:ACOTSR>2.3.CO;2.

Cronin, T., Willard, D., Karlsen, A., Ishman, S., Verardo, S., McGeehin, J., Kerhin, R., Holmes, C., Colman, S., Zimmerman, A., 2000. Climatic variability in the eastern United States over the past millennium from Chesapeake Bay sediments. *Geology*, v. 28, p. 3–6. https://doi.org/10.1130/0091-7613(2000)28%3C3:CVITEU%3E2.0.CO;2.

Cronin, T.M., Dwyer, G.S., Kamiya, T., Schwede, S., Willard, D.A., 2003. Medieval Warm Period, Little Ice Age and 20th century temperature variability from Chesapeake Bay. *Global and Planetary Change*, v. 36, p. 17–29. https://doi.org/10.1016/S0921-8181(02)00161-3.

Davis, E.H., 2020. *A Reassessment of the Late Quaternary Surficial Geology of the Lower Delmarva Peninsula, Virginia*. MSc Thesis: University of Delaware, 107 p. https://www.proquest.com/dissertations-theses/reassessment-late-quaternary-surficial-geology/docview/2445902189/se-2.

Deaton, C.D., Hein, C.J., Kirwan, M.L., 2017. Barrier island migration dominates ecogeomorphic feedbacks and drives salt marsh loss along the Virginia Atlantic Coast, US. *Geology*, v. 45, p. 123–126. https://doi.org/10.1130/G38459.1.

Dolan, R., Hayden, B., Jones, C., 1979. Barrier island configuration, *Science*, v. 204, p. 401–403, https://www.jstor.org/stable/1748387.

Dominguez, R., Fenster, M.S., McManus, J.W., 2024. Storm frequency, magnitude, and cumulative storm beach impact along the US east coast. *Earth Surface Dynamics*, v. 12, p. 1145–1163. https://doi.org/10.5194/esurf-12-1145-2024.

Dowsett, H.J., Robinson, M.M., Foley, K.M., Herbert, T.D., 2021. The Yorktown Formation: Improved stratigraphy, chronology, and paleoclimate interpretations from the U.S. Mid-Atlantic coastal plain. *Geosciences*, v. 11, p. 486. https://doi.org/10.3390/geosciences11120486.

Elko, N., Briggs, T.R., Benedet, L., Robertson, Q., Thomson, G., Webb, B.M., Garvey, K., 2021. A century of US beach nourishment. *Ocean and Coastal Management*, v. 199, p. 105406. https://doi.org/10.1016/j.ocecoaman.2020.105406.

Faunce, K.E., Rapp, J.L., 2020. Topobathymetric digital elevation model (TBDEM) of the eastern shore peninsula of Virginia and adjacent parts of Maryland with horizontal resolution of 1 meter and vertical resolution of 1 centimeter. *US Geological Survey Data Release*. https://www.sciencebase.gov/catalog/item/5e710963e4b01d509268228c.

Fenster, M.S. and FitzGerald, D.M., 2014. A synthesis of field and geographic information systems data from the Virginia Barrier Islands used to test the Conceptual Runaway Barrier Island Transgression Model, *Geological Society of America, Vancouver, BC, Abstracts with Programs*. v. 46, No. 6, p. 484

Fenster, M.S., Bundick, J.A., 2015. Morphodynamics of Wallops Island, Virginia: A mixed-energy, human-modified barrier island, in: McBride, R.A., Fenster, M.S., Seminack, C.T., Richardson, T.M., Sepanik, J.M., Hanley, J.T., Bundick, J.A., Tedder, E. (Eds.), Holocene Barrier-Island Geology and Morphodynamics of the Maryland and Virginia Open-Ocean Coasts: Fenwick, Assateague, Chincoteague, Wallops, Cedar, and Parramore Islands, in: Brezinski, D.K., Halka, J.P., Ortt, J. (Eds.), *Tripping from the Fall Line: Field Excursions for the GSA Annual Meeting, Baltimore, 2015: Geological Society of America Field Guide 40*, Geological Society of America, Boulder, pp. 358–370. https://doi.org/10.1130/2015.0040(10).

Fenster, M.S., Hayden, B.P., 2007. Ecotone displacement trends on a highly dynamic barrier island: Hog Island, Virginia. *Estuaries and Coasts*, v. 30, p. 978–988. https://doi.org/10.1007/BF02841389.

Fenster, M.S., McBride, R.A., 2015. Barrier-island geology and morphodynamics along the open-ocean coast of the Delmarva Peninsula: An Overview, in: McBride, R.A., Fenster, M.S., Seminack, C.T., Richardson, T.M., Sepanik, J.M., Hanley, J.T., Bundick, J.A., Tedder, E. (Eds.), Holocene Barrier-Island Geology and Morphodynamics of the Maryland and Virginia Open-Ocean Coasts: Fenwick, Assateague, Chincoteague, Wallops, Cedar, and Parramore Islands, in: Brezinski, D.K., Halka, J.P., Ortt, J. (Eds.), *Tripping from the Fall Line: Field Excursions for the GSA Annual Meeting, Baltimore, 2015: : Geological Society of America Field Guide 40*, Geological Society of America, Boulder, pp. 310–334. https://doi.org/10.1130/2015.0040(10).

Fenster, M.S., Dolan, R., Smith, J.J., 2016. Grain-size distributions and coastal morphodynamics along the southern Maryland and Virginia barrier islands. *Sedimentology*, v. 63, p. 809–823. https://doi.org/10.1111/sed.12239.

Finkelstein, K., Ferland, M.A., 1987. Back-barrier response to sea-level rise, Eastern Shore of Virginia. In: Nummendal, D., Piley, O.H., Howard, J.D. (Eds.), *Sea-Level Fluctuation and Coastal Evolution*. Society of Economic Paleontologists and Mineralogists Special Publication 41, p. 145–155. https://doi.org/10.2110/pec.87.41.0145.

FitzGerald, D.M., Fenster, M.S., Argow, B.A., Buynevich, I.V., 2008. Coastal impacts due to sea-level rise. *Annual Review of Earth and Planetary Sciences*, v. 36, p. 601–647. https://doi.org/10.1146/annurev.earth.35.031306.140139.

FitzGerald, D.M., Hein, C.J., Hughes, Z., Kulp, M., Georgiou, I., Miner, M., 2018. Runaway barrier island transgression concept: Global case studies, *In:* Moore, L.J., Murray, A.B. (eds), *Barrier Dynamics and the Impact of Climate Change on Barrier Evolution*, Springer, p. 3–56, https://doi.org/10.1007/978-3-319-68086-6_1.

Georgiou, I.Y., Messina, F., Sakib, M.M., Zou, S., Foster-Martinez, M., Bregman, M., Hein, C.J., Fenster, M.S., Shawler, J.L., McPherran, K., Trembanis, A.C., 2023. Hydrodynamics and Sediment-Transport Pathways along a Mixed-Energy Spit-Inlet System: A Modeling Study at Chincoteague Inlet (Virginia, USA), *Journal of Marine Science and Engineering*, v. 11, p. 1075. https://doi.org/10.3390/jmse11051075.

Hapke, C.J., Himmelstoss, E.A., Kratzmann, M., List, J.H., Thieler, E.R., 2011. National assessment of shoreline change: Historical shoreline change along the New England and Mid-Atlantic Coasts. *Open File Report 2010-1118,*

U.S. Geological Survey, Reston, VA, 65 p. https://oaktrust.library.tamu.edu/server/api/core/bitstreams/26962ff8-b600-4b51-954b-0d499ad3beca/content.

Hapke, C.J., Kratzmann, M.G., Himmelstoss, E.A., 2013. Geomorphic and human influence on large-scale coastal change. *Geomorphology*, v. 199, p. 160–170. https://doi.org/10.1016/j.geomorph.2012.11.025.

Hayden, B., 2003. *Annual Number of Storms on the Virginia Coast 1885–2002*. Virginia Coast Reserve Long-Term Ecological Research Project Data Publication 105. https://doi.org/10.6073/pasta/ec6762a03d6595805a31c4d4549c5a9c.

Hayes, M.O., 1979. Barrier island morphology as a function of tidal and wave regime, In: Leatherman, S.P. (Ed.), *Barrier Islands*. Academic Press, New York, pp. 1–28.

Hein, C.J., Shawler, J.L., De Camargo, J.M., Klein, A.H.F., Tenebruso, C., Fenster, M.S., 2019. The role of coastal sediment sinks in modifying longshore sand fluxes: Examples from the coasts of southern Brazil and the Mid-Atlantic USA, In: *Coastal Sediments '19, Proceedings of the 12th International Symposium on Coastal Engineering and Science of Coastal Sediment Processes*, World Scientific Publishing Co., Singapore, p. 2330–2344. https://doi.org/10.1142/9789811204487_0199.

Intergovernmental Panel on Climate Change (IPCC), 2014. Sea level change, In: Stocker, T.F., Qin, D., Plattner, G.-K., Tignor, M., Allen, S.K., Boschung, J., Nauels, A., Xia, Y., Bex, V., Midgley, P.M. (eds.), *Climate Change 2013: The Physical Science Basis. Contribution of Working Group I to the Fifth Assessment Report of the Intergovernmental Panel on Climate Change*: New York, Cambridge University Press, p. 1140–1216, https://doi.org/10.1017/CBO9781107415324.

Jarrett, J.T., 1976. *Tidal Prism - Inlet Area Relationships*. U.S. Army Engineer Waterways Experiment Station, 64 p.

Jones, M., 2016. *Considering Holistic Coastal Response to Climate-Change Induced Shifts in Natural Processes and Anthropogenic Modifications*. MSc Thesis: University of North Carolina, Chapel Hill, 76 p. https://doi.org/10.17615/9av0-ms17.

Kang, X., Xia, M., Pitula, J.S., Chigbu, P., 2017. Dynamics of water and salt exchange at Maryland Coastal Bays. *Estuarine, Coastal and Shelf Science*, v. 189, p. 1–16. https://doi.org/10.1016/j.ecss.2017.03.002.

King, D.B., Jr., Ward, D.L., Hudgins, M.H., Williams, G.G., 2011. *Storm Damage Reduction Project Design for Wallops Island, Version 1.01*: Engineer Research and Development Center, Vicksburg, Mississippi, U.S. Army Corps of Engineers, Report No. ERDC/LAB TR-11-9, 197 p. https://apps.dtic.mil/sti/citations/tr/ADA552352

Kochel, R.C., Kahn, J.H., Dolan, R., Hayden, B.P., May, P.F., 1985. U.S. Mid-Atlantic barrier island geomorphology, *Journal of Coastal Research*, v. 1, p. 1–9. https://www.jstor.org/stable/4297003.

Krantz, D.E., Hobbs, C.H., Wikel, G.L., 2016. Atlantic coast and inner shelf. In: Bailey, C.M., Sherwood, W.C., Eaton, L.S., Powards, D.S., (Eds.), *Geology of Virginia*, Virginia Museum of Natural History, pp. 341–380.

Leatherman, S.P., Rice, T.E., Goldsmith, V., 1982, Virginia barrier island configuration: A reappraisal. *Science*, v. 215, p. 285–287, https://doi.org/10.1126/science.215.4530.285.

Lowery, D.L., 2016. *A Coastal Archaeological Survey and Shoreline Erosion Assessment of Accomack and Northampton Counties, Virginia*. Virginia Department of Historic Resources, Richmond, VA. Unpub. manuscript.

Lowery, D.L., O'Neal, M.A., Wah, J.S., Wagner, D.P., Stanford, D.J., 2010. Late Pleistocene upland stratigraphy of the western Delmarva Peninsula, USA. *Quaternary Science Reviews*, v. 29, p. 1472–1480. https://doi.org/10.1016/j.quascirev.2010.03.007.

Lundine, M., Trembanis, A., 2025. Investigating the origin and dynamics of Carolina Bays. *Marine Geology*, v. 480, p. 107449. https://doi.org/10.1016/j.margeo.2024.107449.

Mariotti, G., Hein, C.J., 2022. Lag in response of coastal barrier-island retreat to sea-level rise. *Nature Geoscience*, v. 15, p. 633–638, https://doi.org/10.1038/s41561-022-00980-9.

McBride, R.A., Fenster, M.S., Seminack, C.T., Richardson, T.M., Sepanik, J.M., Hanley, J.T., Bundick, J.A., Tedder, E. (Eds.), Holocene Barrier-Island Geology and Morphodynamics of the Maryland and Virginia Open-Ocean Coasts: Fenwick, Assateague, Chincoteague, Wallops, Cedar, and Parramore Islands, *in:* Brezinski, D.K., Halka, J.P., Ortt, J. (Eds.), *Tripping from the Fall Line: Field Excursions for the GSA Annual Meeting, Baltimore, 2015: : Geological*

Society of America Field Guide 40, Geological Society of America, Boulder, pp. 310–334. https://doi.org/10.1130/2015.0040(10).

McFarland, E.R., Beach, T.A., 2019. *Hydrogeologic Framework of the Virginia Eastern Shore*. U.S. Geological Survey Scientific Investigations Report 2019-5093, 38 pp. https://doi.org/10.3133/sir20195093.

McPherran, K.A., Dohner, S.M., Trembanis, A.C., 2021. A comparison of the temporal evolution of hydrodynamics and inlet morphology during Tropical Storm Fay, *Shore and Beach*, v. 89, p. 11–22, http://doi.org/10.34237/1008922.

Mixon, R.B., 1985. *Stratigraphic and Geomorphic Framework of Uppermost Cenozoic Deposits in Southern Delmarva Peninsula, Virginia and Maryland*. U.S. Geological Survey Professional Paper 1067-G, 58 pp. https://doi.org/10.3133/pp1067G.

Mixon, R.B., Berquist, C.R. Newell, W.L., Johnson, G.H., 1989. *Geologic Map and Generalized Cross Sections of the Coastal Plain and Adjacent Parts of the Piedmont, Va*. (1:250,000). United States Geological Survey, 2 pp. https://ngmdb.usgs.gov/Prodesc/proddesc_10097.htm.

Murray, B., Ashton, A.D., Coco, G., 2020. From cusps to capes: self-organised shoreline shapes, In: Jackson, D.W.T., Short, A.D (Eds.), *Sandy Beach Morphodynamics*, Elsevier, Amsterdam, pp. 277–295. https://doi.org/10.1016/C2018-0-02420-2.

National Aeronautics and Space Administration (NASA), 2010. *Final Environmental Impact Statement for Wallops Flight Facility Shoreline Restoration and Infrastructure Protection Programs*. Accessed March 2025. https://www.nasa.gov/goddard/memd/nepa/shoreline/.

National Aeronautics and Space Administration (NASA), 2019. *Final NASA Wallops Flight Facility Shoreline Enhancement and Restoration Project Environmental Assessment*. Accessed March 2025. https://www.nasa.gov/goddard/memd/nepa/shoreline/.

National Aeronautics and Space Administration (NASA), 2024. *Wallops Island Shoreline Restoration and Resiliency Programs*. Accessed March 2025. https://www.nasa.gov/goddard/memd/nepa/shoreline/.

Nebel, S.H., Trembanis, A.C., Barber, D.C., 2012. Shoreline analysis and barrier island dynamics: Decadal scale patterns from Cedar Island, Virginia, *Journal of Coastal Research*, v. 280, p. 332–341. https://doi.org/10.2112/JCOASTRES-D-10-00144.1.

Nowacki, D.J., Ganju, N.K., 2018. Storm impacts on hydrodynamics and suspended sediment fluxes in a microtidal back-barrier estuary. *Marine Geology*, v. 404, p. 1–14. https://doi.org/10.1016/j.margeo.2018.06.016.

OCM Partners, 2019. 2015 USGS Lidar: Eastern Shore VA from 2010-06-15 to 2010-08-15. NOAA National Centers for Environmental Information. https://www.fisheries.noaa.gov/inport/item/50784

Oertel, G.F., Foyle, A.M., 1995. Drainage displacement by sea-level fluctuation at the outer margin of the Chesapeake Seaway. *Journal of Coastal Research*, v. 11, p. 583–604. https://www.jstor.org/stable/4298364.

Oertel, G.F., Overman, K., 2004. Sequence morphodynamics at an emergent barrier island, middle Atlantic coast of North America. *Geomorphology*, v. 58, p. 67–83. https://doi.org/10.1016/S0169-555X(03)00187-9.

Oertel. G.F., Kearney, M.S., Leatherman, S.P., Woo, H.-J., 1989. Anatomy of a barrier platform: outer barrier lagoon, southern Delmarva Peninsula, Virginia, In: Ward, L.G., Ashley, G.M. (Eds.), *Physical Processes and Sedimentology of Siliciclastic-Dominate Lagoonal Systems*. Marine Geology, v. 88, p. 303–318. https://doi.org/10.1016/0025-3227(89)90103-5.

Owens, J.P., Denny, C.S., 1979. *Upper Cenozoic deposits of the central Delmarva Peninsula, Maryland and Delaware*. US Geological Survey Professional Paper 1067-A, 32 p. https://pubs.usgs.gov/pp/1067a/report.pdf.

Pendleton, E.A., Williams, S.J., Thieler, E.R., 2004. *Coastal vulnerability assessment of Assateague Island National Seashore (ASIS) to sea-level rise*. Open File Report 2004-1020, U.S. Geological Survey, Reston. https://pubs.usgs.gov/of/2004/1020/html/cvi.htm.

Pickering, J.L., Goodbred Jr, S.L., Beam, J.C., Ayers, J.C., Covey, A.K., Rajapara, H.M., Singhvi, A.K., 2018. Terrace formation in the upper Bengal basin since the Middle Pleistocene: Brahmaputra fan delta construction during multiple highstands. *Basin Research*, v. 30, p. 550–567. https://doi.org/10.1111/bre.12236.

Psuty, N.P., Silveira, T.M., 2011. Monitoring shoreline change along Assateague barrier island: the first trend report. *Journal of Coastal Research*, SI 64, p. 800–804. https://www.jstor.org/stable/26482282.

Raff, J.L., Shawler, J.L., Ciarletta, D.J., Hein, E.A., Lorenzo-Trueba, J., Hein, C.J., 2018. Insights into barrier-island stability derived from transgressive/regressive state changes of Parramore Island, Virginia. *Marine Geology*, v. 403, p. 1–19, https://doi.org/10.1016/j.margeo.2018.04.007.

Railsback, L.B., Gibbard, P.L., Head, M.J., Voarintsoa, N.R.G., Toucanne, S., 2015. An optimized scheme of lettered marine isotope substages for the last 1.0 million years, and the climatostratigraphic nature of isotope stages and substages. *Quaternary Science Reviews*, v. 111, p. 94–106. https://doi.org/10.1016/j.quascirev.2015.01.012.

Ramsey, K.W., 2010. *Stratigraphy, Correlation, and Depositional Environments of the Middle to Late Pleistocene Interglacial Deposits of Southern Delaware*. Newark, DE, 50 p. http://udspace.udel.edu/handle/19716/5416.

Rice, T.E., Leatherman, S.P., 1983. Barrier island dynamics: The Eastern Shore of Virginia. *Southeastern Geology*, v. 24, p. 125–137. https://southeasterngeology.org/wp-content/uploads/2020/08/Vol.-24-N.-3-November-1983.pdf.

Rice, T.E., Niedoroda, A.W., Pratt, A.P., 1976. *Coastal Processes and Geology: Virginia Barrier Islands*. The Virginia Coast Reserve Study: Arlington, Virginia, The Nature Conservancy, p. 109–382. https://repository.library.noaa.gov/view/noaa/2214.

Richardson, T.M., 2012. *Morphodynamic Changes of the Parramore-Cedar Barrier Island System and Wachapreague Inlet, Virginia from 1852 to 2011: A Model of Barrier Island and Tidal Inlet Evolution Along the Southern Delmarva Peninsula, USA*. Ph.D. thesis: Fairfax, George Mason University, 306 p. https://www.proquest.com/openview/bcfa4d607f620bf7ebb9ac80cd0280a2/1?cbl=18750&pq-origsite=gscholar.

Richardson, T.M., McBride, R.A., 2007. Historical shoreline changes and morphodynamics of Parramore Island, Virginia (1852–2006), In: Kraus, N.C., Rosati, J.D. (eds.), *Proceedings of Coastal Sediments 2007*: American Society of Civil Engineers, v. 1, p. 364–377, https://doi.org/10.1061/40926(239)28.

Richardson, T.M., McBride, R.A., 2011. Historical shoreline changes and morphodynamics of Cedar Island, Virginia, USA: 1852–2010, In: Kraus, N.C., Rosati, J.D. (eds.), *Proceedings of Coastal Sediments 2011*: World Scientific Publishing Co., v. 2, p. 1285–1298. https://doi.org/10.1142/9789814355537_0097.

Rick, T., Barber, M., Lowery, D., Wah, J., Madden, M., 2015. Early Woodland Coastal Foraging at the Savage Neck Shell Midden (44NH478), Chesapeake Bay, Virginia. *Archaeology of Eastern North America*, v. 43, p. 23–38. https://www.jstor.org/stable/43868968.

Robbins, M.G., Shawler, J.L., Hein, C.J., 2022. Contribution of longshore sand exchanges to mesoscale barrier-island behavior: Insights from the Virginia Barrier Islands, US East Coast. *Geomorphology*, v. 403, p. 108163, https://doi.org/10.1016/j.geomorph.2022.108163.

Sallenger, A.H., Jr., Doran, K.S., Howd, P.A., 2012. Hotspot of accelerated sea-level rise on the Atlantic coast of North America. *Nature Climatic Change*, v. 2, p. 884–888, https://doi.org/10.1038/NCLIMATE1597.

Shawler, J.L., Ciarletta, D.J., Lorenzo-Trueba, J., Hein, C.J., 2019. Drowned foredune ridges as evidence of pre-historical barrier-island state changes between migration and progradation, In: Wang, P., Rosati, J., Valiee, M., (Eds.), *Coastal Sediments '19: Proceedings of the 12th International Symposium on Coastal Engineering and Science of Coastal Sediment Processes*, World Scientific, Tampa/St. Petersburg, pp. 158–171. https://doi.org/10.1142/9789811204487_0015.

Shawler, J.L., Ciarletta, D.J., Connell, J.E., Boggs, B.Q., Lorenzo-Trueba, J., Hein, C.J., 2021a. Relative influence of antecedent topography and sea-level rise on barrier-island migration. *Sedimentology*, v. 68, p. 639–669. https://doi.org/10.1111/sed.12798.

Shawler, J.L., Hein, C.J., Obara, C.A., Robbins, M.G., Huot, S., Fenster, M.S., 2021b. The effect of coastal landform development on decadal-to millennial-scale longshore sediment fluxes: Evidence from the Holocene evolution of the central mid-Atlantic coast, USA, *Quaternary Science Reviews*, v. 267, p. 107096. https://doi.org/10.1016/j.quascirev.2021.107096.

Shawler, J.L., Hein, C.J., Sakib, M.M., Messina, F., Georgiou, I.Y., 2025. Local versus regional controls on the morphology and texture of preserved beach and foredune ridges, *Journal of Geophysical Research: Earth Surface*. v. 130, p. e2025JF008429. https://doi.org/10.1029/2025JF008429.

Stahle, D.W., Cleaveland, M.K., 1994. Tree-ring reconstructed rainfall over the southeastern U.S.A. during the Medieval Warm Period and Little Ice Age. *Climatic Change,* v. 26, p. 199–212. https://doi.org/10.1007/BF01092414.

Swift, D.P., Parson, B.S., Foyle, A., Oertel, G.F., 2003. Between beds and sequences: Stratigraphic organization at intermediate scales in the Quaternary of the Virginia coast, USA. *Sedimentology*, v. 50, p. 81–111. https://doi.org/10.1046/j.1365-3091.2003.00540.x.

Thomas, C.W., Murray, A.B., Ashton, A.D., Hurst, M.D., Barkwith, A.K., Ellis, M.A., 2016. Complex coastlines responding to climate change: do shoreline shapes reflect present forcing or "remember" the distant past?. *Earth Surface Dynamics*, v. 4, p. 871–884. https://doi.org/10.5194/esurf-4-871-2016.

U.S. Army Corps of Engineers, 2018. *Wallops Island, VA Shoreline Mapping Program Beach Profile Monitoring Survey Evaluation, Final Report, Fall 2017*. https://netspublic.grc.nasa.gov/main/WFF%20SERP%20EA__V3.pdf.

U.S. Fish & Wildlife Service (USFWS) 2024. *Beach Relocation Background Slide Show*, created for public information session on September 25, 2024. https://www.fws.gov/carp/media/beach-relocation-background-slide-show

U.S. Geological Survey (USGS) 2016. Topobathymetric model for Chesapeake Bay region - District of Columbia, States of Delaware, Maryland, Pennsylvania, and Virginia, 1859 to 2015, 1st edition. https://www.fisheries.noaa.gov/inport/item/55321.

Walters, D., Moore, L.J., Duran Vinent, O., Fagherazzi, S., Mariotti, G., 2014. Interactions between barrier islands and backbarrier marshes affect island system response to sea level rise: Insights from a coupled model. *Journal of Geophysical Research: Earth Surface*, v. 119, p. 2013–2031. https://doi.org/10.1002/2014JF003091.

Ward, L.W., Blackwelder, B.W., 1980. *Stratigraphic Revision of Upper Miocene and Lower Pliocene Beds of the Chesapeake Group, Middle Atlantic Coastal Plain*. Geological Survey Bulletin 1482-D, US Government Printing Office, 80 p. https://pubs.usgs.gov/bul/1482d/report.pdf.

Wei, E., Miselis, J., 2023. Shoreface sediment availability offshore of a rapidly migrating, mixed-energy barrier island. In: *Coastal Sediments '23, Proceedings of the 13th International Symposium on Coastal Engineering and Science of Coastal Sediment Processes*, World Scientific Publishing Co., Singapore, p. 2309-2916. https://doi.org/10.1142/9789811275135_0215.

Wikel, G.L., 2008. *Variability in Geologic Framework and Shoreline Change: Assateague and Wallops Islands, Eastern Shore of Virginia*. M.S. Thesis: Virginia Institute of Marine Science, William & Mary, 210 p. https://scholarworks.wm.edu/handle/internal/4682.

Willard, D.A., Cronin, T.M., Verardo, S., 2003. Late-Holocene climate and ecosystem history from Chesapeake Bay sediment cores, USA. *The Holocene,* v. 13, p. 201–214. https://doi.org/10.1191/0959683603hl607rp.

Wilson, I.T., Tuberville, T., 2003. *Virginia's Precious Heritage: A Report on the Status of Virginia's Natural Communities, Plants, and Animals, and a Plan for Preserving Virginia's Natural Heritage Resources*. Natural Heritage Technical Report (No. 03-15). Virginia Department of Conservation and Recreation, Division of Natural Heritage, Richmond, Virginia, 82 p. https://www.dcr.virginia.gov/natural-heritage/document/nhpc-web.pdf.

Wright, L.D., Boon, J.D., Green, M.O., List, J.H., 1986. Response of the mid shoreface of the southern Mid-Atlantic Bight to a "northeaster". *Geo-Marine Letters*, v. 6, p. 153-160. https://doi.org/10.1007/BF02238086.